NTNU
Norwegian University of
Science and Technology

State Estimation and Kalman Filtering of Tethered Airfoils

by use of ground based meausrments

Ola Holter Hjukse

Master of Science in Engineering Cybernetics
Submission date: June 2011
Supervisor: Tor Arne Johansen, ITK

Norwegian University of Science and Technology
Department of Engineering Cybernetics

Abstract

This thesis contains modeling, observability analysis and state estimator design of a tethered airfoil. A existing model is extended to include wind dynamics. The observability analysis shows that the system is indeed observable. A comparison is made between Extended and Unscented Kalman filter (UKF) and the UKF is found to achieve best results during simulations.

Acknowledgements

I would like to thank Håvard Knappskog, Tor-Arne Johnansen and Jan Hystad for the help and assistance provided. I would also like to thank the guys at the faculty engineering workshop for help with all the practical issues.

Contents

List of Figures

List of Tables

GLOSSARY

Glossary

α_{UKF}	UKF tuning parameter determining the spread of sigma points around mean
α_{wind}	Wind shear power law exponent
α_w	Pitch angle [rad]
β_b	Body frame orientation in local frame [rad]
β_{UKF}	UKF tuning parameter incorporating prior knowledge of distribution of the states
β_w	Yaw angle [rad]
δ_l	Flaps angle [rad]
γ	Wind orientation in earth frame [rad/s]
χ	Sigma points
$\hat{\mathbf{x}}$	Estimated state vector
$\hat{\mathbf{y}}$	Estimated measurement vector
υ	Wind vector given in Cartesian coordinates
$\mathbf{B}$	Kite model input function
$\mathbf{F}$	Kite model function
$\mathbf{f}_{w,t}$	The wind turbulence function
$\mathbf{H}$	Measurements function
$\mathbf{K}$	EKF Kalman gain
$\mathbf{P}$	Error covariance matrix
$\mathbf{Q}$	State noise covariance matrix
$\mathbf{q}_w^e$	Wind vector at height h_0
$\mathbf{q}_w$	Wind vector
$\mathbf{R}$	Measurement noise covariance matrix
$\mathbf{x}$	State vector
$\mathbf{y}$	Measurement vector
$\mathcal{K}$	UKF Kalman gain
μ	Wind orientation in earth frame [rad/s]
ν	Wind strength [m/s]
ϕ	Spherical coordinate [rad]
$\sigma_{y,x,z}$	Turbulence intensities
θ	Spherical coordinate [rad]
C_k	Directional stability of the kite
F^l	Sum of forces in the local system

GLOSSARY

F^l_{aer}	Aerodynamic forces acting on the kite in the local system
F^l_g	Forces caused by gravity acting on the kite in the local system
L	Number of states in the system
M_k	Yawing moment of kite
R^b_l	Transformation matrix from body- to local-system
R^l_e	Transformation matrix from local- to earth-system
R^w_b	Transformation matrix from wind- to body-system
v	Measurement noise
w	State noise
EKF	Extended Kalman filter
GRV	Gaussian Random Variable
KF	Kalman Filter
MSE	Mean Squared Error
PDF	Probability Density Function
UKF	Unscented Kalman filter, also known as Sigma-point Kalman filter

1

Introduction

1.1 Motivation

The use of kites as a propulsion device is not a new idea. Even so it has since the introduction of the combustion motor, been seen more as novelty item than as a serious way of propulsion or power generation. This is changing as kites used to aid propulsion of large vessel such as cargo ships [1], as well as many serious concepts of power generation, has grown popular the recent years. [5, 10, 8, 15, 16] The main advantages of using kite to generate power as opposed to windmills is that the windmill power generation capabilities is bounded by the size of its blades and the height of the construction. Kites does not have that problem as they do not need a big ground structure and are able to operate at greater heights where the wind speed is greater [17]. This have lead to many concepts dealing with kites for use in power generation. In these concepts it is often assumed that measurements of all necessary states are readily available, and therefor involves measuring the kite position, speed and rotation using different measuring devices attached to the kite itself. This impose challenges such as added weight and the need for communication between the kite-based measuring device and the controller.

This thesis explores the concept of estimating the state of the kite using ground based measurements. These measurements are typically the angle between the ground and the cable (θ), the rotational angle around the z-axis (ϕ), the wind at ground level, and the the effect of the control lines as depicted in Figure 1.1.

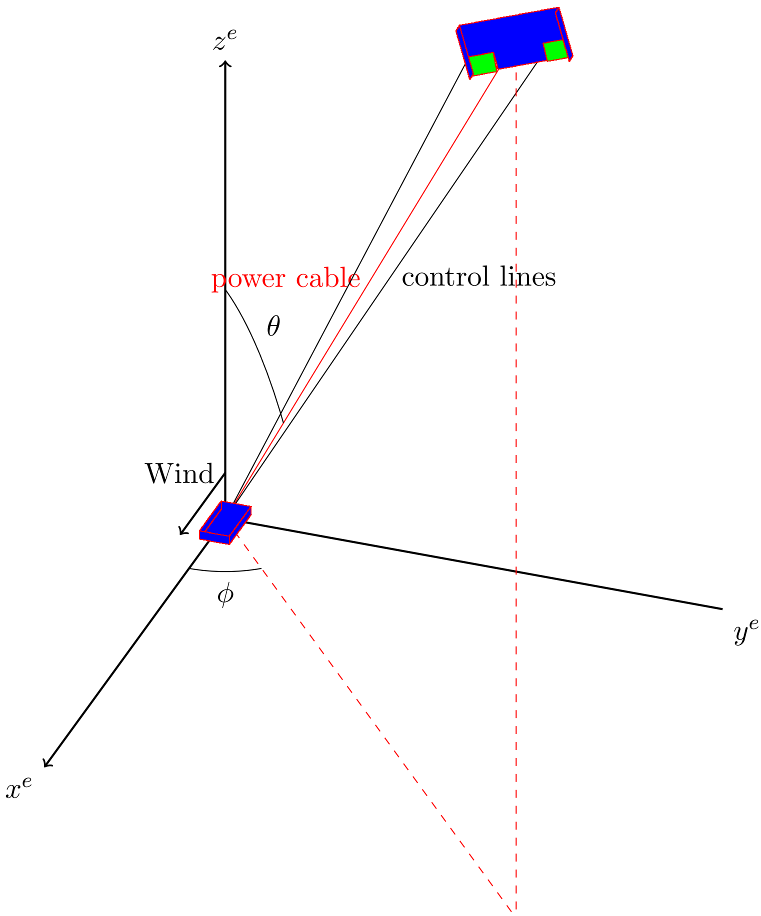

Figure 1.1: The kite and the ground based control and measurement unit

1.2 Outline

The outline of the thesis:

- Kite modeling
- Wind modeling
- Observability analysis
- State estimation
- Simulation
- Conclusion
- Discussion and further work

2

Kite Modeling

The first part of this chapter (2.1) is a brief summary of the kite model given in Håvard Knappskog's Master thesis "Nonlinear control of tethered airfoils" [12]. The model is the discretized in 2.2.

2.1 Continuous model

The kinematics of the kite system is based on Euler Lagrange's equation of motion, with $q = (\theta, \phi, r)^T$ being the spherical coordinates:

$$\frac{d}{dt}\left(\frac{\partial L}{\partial \dot{q}_i}\right) - \frac{\partial L}{\partial q_i} = \tau_i \tag{2.1}$$

and the Lagrangian L is given by:

$$L(q, \dot{q}, t) = T(q, \dot{q}, t) - U(q) \tag{2.2}$$

$$T_{kin} = \frac{1}{2}\overline{m}|\dot{p}|^2 = \frac{\overline{m}}{2}\left(\dot{r}^2 + r^2\sin(\theta)\dot{\phi}^2 + r^2\dot{\theta}^2\right) \tag{2.3}$$

$\overline{m}$ is the mass of the system assumed only to be the mass of the kite: $\overline{m} = m$. T is the kinetic energy and U is the potential energy given by:

$$U = mgh = mgr\cos(\theta) \tag{2.4}$$

The following is derived from the above equations::

$$\ddot{q} = S^{-1}\frac{F^l}{m} - a \tag{2.5}$$

Which is the final continuous model. F^l is the sum of forces given in the local frame.S is a scaling matrix given by:

$$S = \begin{pmatrix} r & 0 & 0 \\ 0 & r\sin(\theta) & 0 \\ 0 & 0 & 0 \end{pmatrix} \tag{2.6}$$

and a is the pseudo force:

$$a = \begin{pmatrix} 2\frac{\dot{r}}{r}\dot{\theta} - \sin(\theta)\cos(\theta)\dot{\phi}^2 \\ 2\frac{\dot{r}}{r}\dot{\phi} + 2\frac{\cos(\theta)}{\sin(\theta)}\dot{\theta}\dot{\phi} \\ -r\sin(\theta)\dot{\phi}^2 - r\dot{\theta}^2 \end{pmatrix} \tag{2.7}$$

The sum of the forces given in the local system consists of:

$$F^l = F^l_g + F^l_{aer} + F^l_c \tag{2.8}$$

where F^l_g is the force caused by gravity:

$$F^l_g = m\begin{pmatrix} g\sin(\theta) \\ 0 \\ -g\cos(\theta) \end{pmatrix} \tag{2.9}$$

F^l_{aer} is the aerodynamic forces and F^l_c is the cable force:

$$F^l_c = -\left(F^l_g + F^l_{aer}\right)_3 \tag{2.10}$$

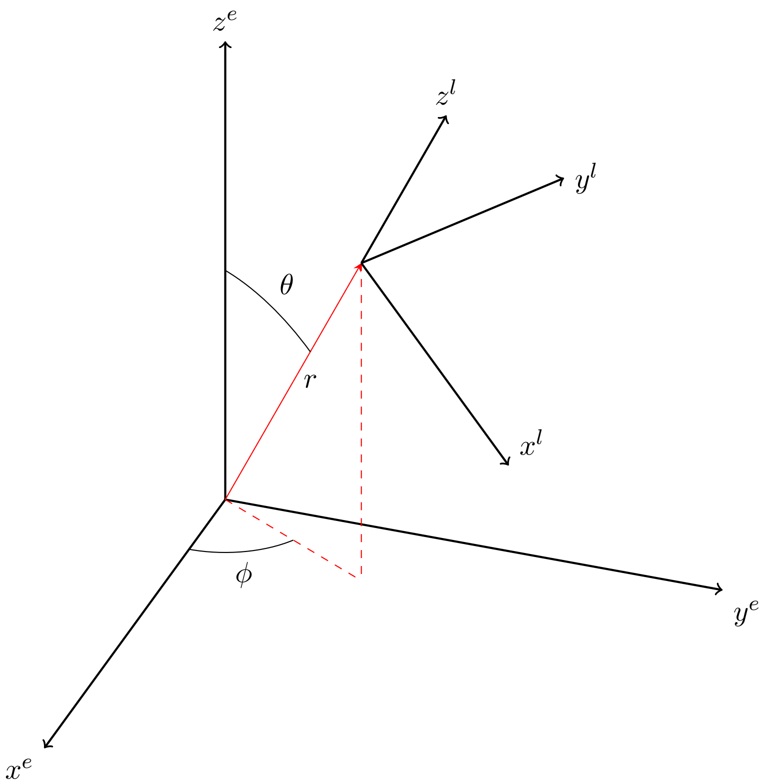

Figure 2.1: The earth and local coordinate systems. The spherical coordinates $q = (\theta, \phi, r)^T$ is indicated in the figure

Such that the sum of the forces in e_r-direction is zero, $F_3^l = 0$. $\ddot{q}$ is then given by:

$$\ddot{\theta} = \frac{F_\theta}{mr} - a_\theta \tag{2.11}$$

$$\ddot{\phi} = \frac{F_\phi}{mr\sin(\theta)} - a_\phi \tag{2.12}$$

$$\ddot{r} = \frac{F_r}{m} - a_r \tag{2.13}$$

By assuming r to be constant and adding the yaw of the kite body around the cable β_b, and the flaps angle δ_l as states the kite model is given by:

$$\begin{pmatrix} \ddot{\theta} \\ \ddot{\phi} \\ \ddot{\beta}_b \\ \dot{\delta}_l \end{pmatrix} = \begin{pmatrix} \left(S^{-1}\frac{F^l}{m} - a\right)_1 \\ \left(S^{-1}\frac{F^l}{m} - a\right)_2 \\ \frac{M_k}{I_k} \\ b_u u \end{pmatrix} \tag{2.14}$$

M_k is the yawing moment and is given by:

$$M_k = \frac{1}{2}\rho_{air}(q_w)^2 bAC_k - c_{kd}\dot{\beta}_b \tag{2.15}$$

where q_w is the relative wind to the kite and C_k is the sum of the natural directional stability of the kite and the control input:

$$C_k = -c_{ks}\beta_s + c_{k,+delta_c}\delta_l \tag{2.16}$$

2.1.1 Coordinate frames and transformation matrices

The following right-handed orthogonal reference frames with corresponding unit vectors in the x-, y- and z-direction are defined as:

- Earth frame, unit vectors: e_x, e_y and e_z, shown in Figure 2.2

- Local frame, unit vectors: e_θ, e_ϕ and e_r, shown in Figure 2.2
- Body frame, unit vectors: e_i, e_j and e_k, shown in Figure 2.2
- Wind frame, unit vectors: e_w, e_t and e_n, shown in Figure 2.3

The relationship between the coordinate frames are given by transformation matrices which makes it possible to relate information given in one coordinate frame to another.

The transformation matrix from the local- to the earth-frame is given by:

$$\begin{aligned} R_e^l =& R_y(\theta)R_z(\phi) \\ =& \begin{pmatrix} \cos(\theta)\cos(\phi) & \cos(\theta)\sin(\phi) & -\sin(\theta) \\ -\sin(\phi) & \cos(\phi) & 0 \\ \sin(\theta)\cos(\phi) & \sin(\theta)\sin(\phi) & \cos(\theta) \end{pmatrix} \end{aligned} \tag{2.17}$$

The transformation matrix from the body- to the local-frame is given by:

$$\begin{aligned} R_l^b =& R_z(\beta_b) \\ =& \begin{pmatrix} \cos(\beta_b) & \sin(\beta_b) & 0 \\ -\sin(\beta_b) & \cos(\beta_b) & 0 \\ 0 & 0 & 1 \end{pmatrix} \end{aligned} \tag{2.18}$$

The transformation matrix from the wind- to the body-frame is given by:

$$\begin{aligned} R_b^w =& R_y(\alpha_w)R_z(\beta_w) \\ =& \begin{pmatrix} \cos(\alpha_w)\cos(\beta_w) & \cos(\alpha_w)\sin(\beta_w) & -\sin(\alpha_w) \\ -\sin(\beta_w) & \cos(\beta_w) & 0 \\ \sin(\alpha_w)\cos(\beta_w) & \sin(\alpha_w)\sin(\beta_w) & \cos(\alpha_w) \end{pmatrix} \end{aligned} \tag{2.19}$$

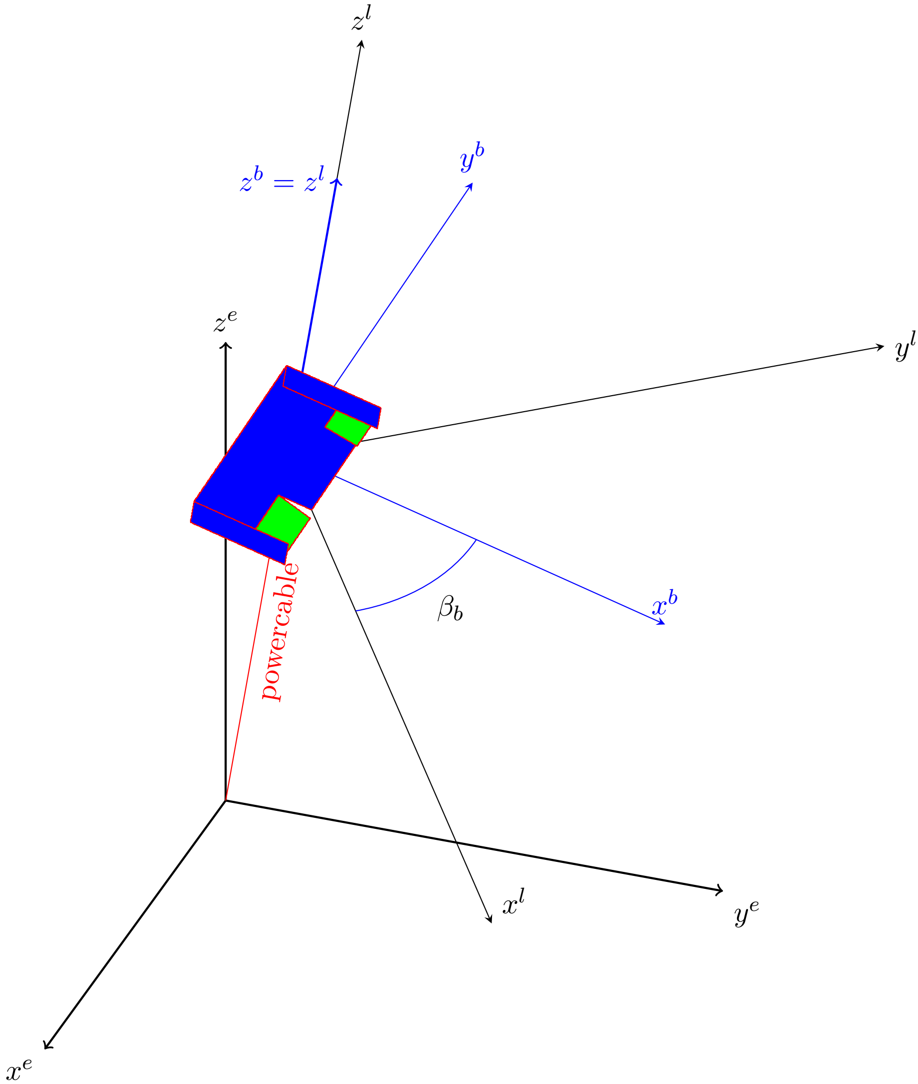

Figure 2.2: The local frame and the body frame. The body frame orientation around the local frame β_b is indicated in the figure.

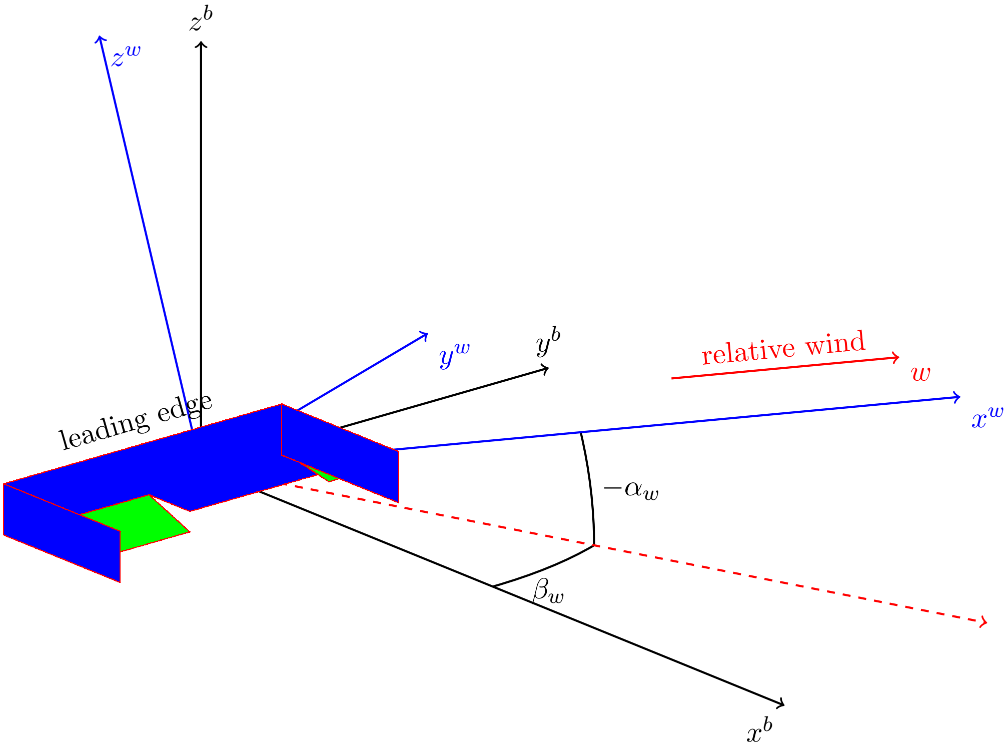

Figure 2.3: The body frame and the wind frame. The relative wind, the yaw-angle β_w and the pitch angle α_w is indicated in the figure.

The yaw-angle β_w and the pitch angle α_w (indicated in Figure 2.3) is the product of the states and the wind vector, and is therefor unknown. However, by defining the relative wind vector υ given in the local frame, it is possible to calculate α_w and β_w

$$\begin{aligned}
\upsilon_e^l =& R_e^l \upsilon^e - \dot{p}^l \\
=& \begin{pmatrix} c(\theta)c(\phi) & c(\theta)s(\phi) & -s(\theta) \\ -s(\phi) & c(\phi) & 0 \\ s(\theta)c(\phi) & s(\theta)s(\phi) & c(\theta) \end{pmatrix} \begin{pmatrix} \upsilon_x \\ \upsilon_y \\ \upsilon_z \end{pmatrix} - \begin{pmatrix} r\dot{\theta} \\ rs(\theta)\dot{\phi} \\ 0 \end{pmatrix} && (2.20) \\
=& \begin{pmatrix} c(\theta)c(\phi)\upsilon_x + c(\theta)s(\phi)\upsilon_y - s(\theta)\upsilon_z - r\dot{\theta} \\ -s(\phi)\upsilon_x + c(\phi)\upsilon_y - rs(\theta)\dot{\phi} \\ s(\theta)c(\phi)\upsilon_x + s(\theta)s(\phi)\upsilon_y + c(\theta)\upsilon_z \end{pmatrix} && (2.21)
\end{aligned}$$

it is assumed that $\dot{r} = 0$ and the wind vector is dominated by wind along the x^e-axis. It is now possible to show that α_w and β_w are given by [12]:

$$\alpha_w = -\arcsin\left(\frac{\upsilon_x s(\theta)c(\phi)}{\sqrt{(\upsilon_x c(\theta)c(\phi) - r\dot{\theta})^2 + (\upsilon_x s(\phi) + rs(\theta)\dot{\phi})^2 + (\upsilon_x s(\theta)c(\phi))^2}}\right) \tag{2.22}$$

$$\beta_s = -\arcsin\left(\frac{c(\beta_b)(\upsilon_x s(\phi) + rs(\theta)\dot{\phi}) + s(\beta_b)(\upsilon_x c(\theta)c(\phi) - r\dot{\theta})}{\sqrt{(\upsilon_x c(\theta)c(\phi))^2 + (\upsilon_x s(\phi) + rs(\theta)\dot{\phi})^2}}\right) \tag{2.23}$$

2.1.2 State space representation of the system

By using the results of the previous chapters the kite model is represented by the following state space model:

$$\dot{\mathbf{x}} = \mathbf{f}(\mathbf{x}, \upsilon, t) + u(t) + \mathbf{w}(t) \tag{2.24}$$

$$\mathbf{y} = \mathbf{h}(\mathbf{x}, t) + \mathbf{v}(t) \tag{2.25}$$

where:

$$\mathbf{x} = \begin{bmatrix} \theta \\ \phi \\ \beta_b \\ \dot{\theta} \\ \dot{\phi} \\ \dot{\beta}_b \\ \delta_l \end{bmatrix} \tag{2.26}$$

The system is then given by:

$$\begin{bmatrix} \dot{x_1} \\ \dot{x_2} \\ \dot{x_3} \\ \dot{x_4} \\ \dot{x_5} \\ \dot{x_6} \\ \dot{x_7} \end{bmatrix} = \begin{bmatrix} x_4 \\ x_5 \\ x_6 \\ \left(S^{-1}\frac{F^l}{m} - a\right)_1 \\ \left(S^{-1}\frac{F^l}{m} - a\right)_2 \\ \frac{M_k}{I_k} \\ 0 \end{bmatrix} + \begin{bmatrix} 0 \\ 0 \\ 0 \\ 0 \\ 0 \\ 0 \\ b_u \end{bmatrix} u + \begin{bmatrix} w_{x_4} \\ w_{x_5} \\ w_{x_6} \\ w_{\dot{x_4}} \\ w_{\dot{x_5}} \\ w_{\dot{x_6}} \\ w_{\dot{x_7}} \end{bmatrix} \tag{2.27}$$

2.2 Discretization of the system

If the model is to be used to control and/or monitor hardware, it is necessary to discretize the system. The discretization is achieved by using the Euler first order method and the discrete system is given by:

$$\begin{aligned}
\mathbf{x}_k =& \mathbf{x}_{k-1} + h \cdot (\mathbf{f}(\mathbf{x}_{k-1}, \upsilon, t) + u_k + \mathbf{w}) \\
\begin{bmatrix} x_{1,k} \\ x_{2,k} \\ x_{3,k} \\ x_{4,k} \\ x_{5,k} \\ x_{6,k} \\ x_{7,k} \end{bmatrix} =& \begin{bmatrix} x_{1,k-1} \\ x_{2,k-1} \\ x_{3,k-1} \\ x_{4,k-1} \\ x_{5,k-1} \\ x_{6,k-1} \\ x_{7,k-1} \end{bmatrix} + h \cdot \left(\begin{bmatrix} x_{4,k-1} \\ x_{5,k-1} \\ x_{6,k-1} \\ \dot{x}_{4,k-1} \\ \dot{x}_{5,k-1} \\ \dot{x}_{6,k-1} \\ 0 \end{bmatrix} + \begin{bmatrix} 0 \\ 0 \\ 0 \\ 0 \\ 0 \\ 0 \\ b_u \end{bmatrix} u_k + \begin{bmatrix} w_{x_4} \\ w_{x_5} \\ w_{x_6} \\ w_{\dot{x_4}} \\ w_{\dot{x_5}} \\ w_{\dot{x_6}} \\ w_{\dot{x_7}} \end{bmatrix} \right)
\end{aligned} \tag{2.28}$$

Where h is the step size given by the sampling frequency.

3

Wind Modeling

When modeling the influence of wind on a kite there are two main factors which needs to be considered, namely:

- Change in wind speed due to altitude and terrain (wind shear).
- Effect of wind turbulence.

In section 3.1 the effect of altitude and ground terrain on the wind speed is introduced while a way of modeling the turbulence is introduced in section 3.2.

3.1 Wind Shear Modeling

One of the main advantages of using kites to generate power is their ability operate at higher altitudes than conventional windmills as the wind velocity

$\upsilon \in \mathbb{R}^3$ increases with altitude $h \in \mathbb{R}$ with a factor given by: [17]

$$\upsilon(h) = \upsilon^e \left(\frac{h}{h_0}\right)^{\alpha_{wind}} \tag{3.1}$$

where $\upsilon^e \in \mathbb{R}^3$ is the wind velocity at a given altitude $h_0 \in \mathbb{R}$ and $\alpha_{wind} \in \mathbb{R}$ is the power law exponent. The height of the kite h is given by the measured angle θ:

$$h = r\cos(\theta) \tag{3.2}$$

α_{wind} varies with the terrain and is found empirically. Typically used values of α_{wind} is found in table 3.1 [17].

Terrain Description	$\alpha_{\mathbf{wind}}$
Smooth, hard ground, lake or ocean	0.10
Short grass on untilled ground	0.14
Level country with foot-high grass, occasional tree	0.16
Tall row crops, hedges, a few trees	0.20
Many trees and occasional buildings	0.22-0.24
Wooded country - small towns and suburbs	0.28-0.30
Urban areas with tall buildings	0.4

Table 3.1: Typical wind power law exponents for varying terrain

In this paper α_{wind} is set to $\frac{1}{7} \approx 0.14$ as the terrain is relative smooth in the areas of interest for installation of the kite controller. Figure 3.1 shows the the altitude dependent wind velocity with $\alpha_{wind} = \frac{1}{7}$.

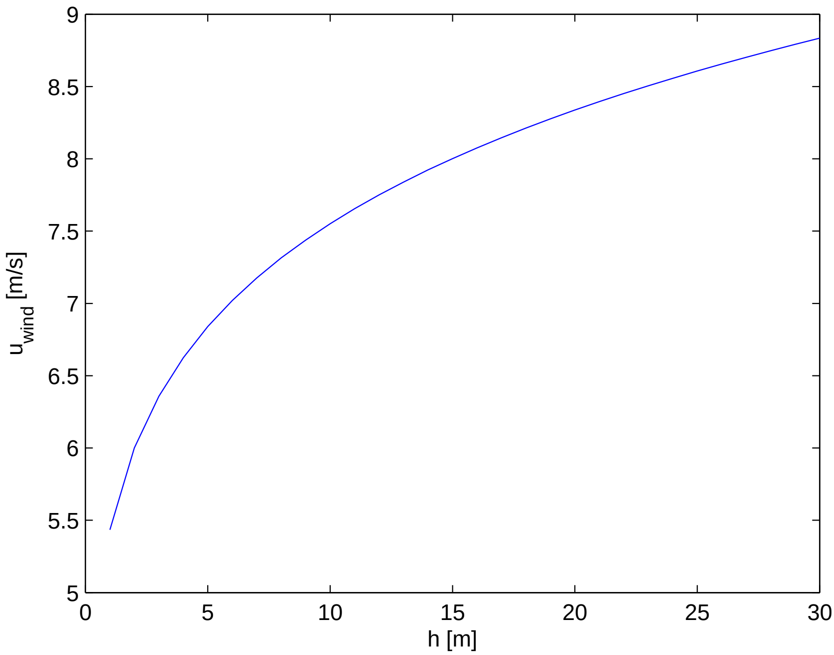

Figure 3.1: Wind shear - Wind velocity at different heights with $\upsilon^e = [6, 0, 0]$ [m/s] and $h_0 = 2$ [m]

3.2 Wind Turbulence modeling

The total wind contribution is given by a vector consisting of contributions from the stable wind $\upsilon \in \mathbb{R}^3$ and the turbulence $\delta\upsilon \in \mathbb{R}^3$.

$$\upsilon_{total} = \upsilon + \delta\upsilon \tag{3.3}$$

Turbulence is defined as irregular fluctuation of the speed, in this case wind speed, at any point from instant to instant about a mean value. [6, 7] The turbulence is therefor assumed to be a random process with the expectation value $E\{\delta\upsilon\} = 0$. [10]

The autocorrelation function $\mathbf{K} : \mathbb{R} \times \mathbb{R} \rightarrow \mathbb{R}^{3\times 3}$ of the turbulence $\delta\upsilon$ is given by

$$\mathbf{K}(t,\tau) = \mathbb{E}\{[\delta\upsilon(t)][\delta\upsilon(t)]^T\} \tag{3.4}$$

$$\mathbf{K}(t,\tau) = \mathbf{K}(\tau,t)^T \tag{3.5}$$

$$\forall t,\tau \in \mathbb{R}$$

The power spectral density $\mathbf{S} : \mathbb{R} \times \mathbb{R} \rightarrow \mathbb{R}^{n_{\upsilon_{total}} \times n_{\upsilon_{total}}}$ of the turbulence is defined to be the Fourier transform of the autocorrelation function;

$$\mathbf{S}(t,\omega) := \int_{-\infty}^{\infty} \mathbf{K}(t,\tau) e^{-i\omega(t-\tau)} d\tau \qquad \forall t,\omega \in \mathbb{R} \tag{3.6}$$

where t is the time and ω is the frequency.

A simplified version of Dryden's wind turbulence model is given by [10, 6]:

$$\mathbf{S}(t,\omega) = \begin{pmatrix} \frac{2\sigma_x^2\delta}{\delta^2+\omega^2} & 0 & 0 \\ 0 & \sigma_y^2\delta\frac{\delta^2+3\omega^2}{(\delta^2+\omega^2)^2} & 0 \\ 0 & 0 & \sigma_z^2\delta\frac{\delta^2+3\omega^2}{(\delta^2+\omega^2)} \end{pmatrix} \qquad \forall t,\omega \in \mathbb{R} \tag{3.7}$$

where $\sigma_x, \sigma_y, \sigma_z \in \mathbb{R}$ are the turbulence intensities and $\delta \in \mathbb{R}$ is the correlation rate.

The corresponding autocorrelation $\mathbf{K}$ is given by:

$$\mathbf{K}(t,\tau) = \begin{pmatrix} \sigma_x^2 & 0 & 0 \\ 0 & \sigma_y^2\left(1 - \frac{|\tau'|}{2}\right) & 0 \\ 0 & 0 & \sigma_z^2\left(1 - \frac{|\tau'|}{2}\right) \end{pmatrix} e^{-|\tau'|} \tag{3.8}$$

$$\tau' = (t-\tau)\delta \quad \forall t, \tau, \tau' \in \mathbb{R}$$

It is possible to simulate the wind turbulence with the above autocorrelation function by passing white noise through a sequence of linear forming filters. One way of simulating the turbulence is described in Appendix A

3.3 Kite model with wind added as process states

The wind vector v_{total} found in 3.2 is given in Cartesian coordinates. Before adding wind as process states a conversion from Cartesian to spherical coordinates is carried out.

$$\begin{aligned}
\nu_{total} =& \sqrt{x^2 + y^2 + z^2} \\
=& \sqrt{(\upsilon + \delta\upsilon)_x^2 + (\upsilon + \delta\upsilon)_y^2 + (\upsilon + \delta\upsilon)_z^2}
\end{aligned} \tag{3.9}$$

$$\begin{aligned}
\gamma_{total} =& \arccos\left(\frac{z}{r}\right) \\
=& \arccos\left(\frac{(\upsilon + \delta\upsilon)_z}{\nu_{total}}\right)
\end{aligned} \tag{3.10}$$

$$\begin{aligned}
\mu_{total} =& \arctan\left(\frac{y}{x}\right) \\
=& \arctan\left(\frac{(\upsilon + \delta\upsilon)_y}{(\upsilon + \delta\upsilon)_x}\right)
\end{aligned} \tag{3.11}$$

The new states added to the system μ, γ and ν as well as the contribution of the turbulence w_ν, w_γ and w_μ is given by:

$$\nu = \sqrt{(\upsilon)_x^2 + (\upsilon)_y^2 + (\upsilon)_z^2} \tag{3.12}$$

$$w_\nu = \sqrt{(\delta\upsilon)_x^2 + (\delta\upsilon)_y^2 + (\delta\upsilon)_z^2} \tag{3.13}$$

$$\gamma = \arccos\left(\frac{(\upsilon)_z}{\nu}\right) \tag{3.14}$$

$$w_\gamma = \arccos\left(\frac{(\upsilon)_z}{\sqrt{(\delta\upsilon)_x^2 + (\delta\upsilon)_y^2 + (\delta\upsilon)_z^2}}\right) \tag{3.15}$$

$$\mu = \arctan\left(\frac{(\upsilon)_y}{(\upsilon)_x}\right) \tag{3.16}$$

$$w_\mu = \arctan\left(\frac{(\delta\upsilon)_y}{(\delta\upsilon)_x}\right) \tag{3.17}$$

where ν is the strength of the wind, γ and μ is the direction of the wind as shown in Figure 3.2 while w_μ, w_γ and w_ν is the influence of the turbulence on strength and direction of the wind.

The effective wind on the local system is then given by:

$$\mathbf{q}_w = \begin{bmatrix} \nu \\ \gamma \\ \mu \end{bmatrix}$$

$$= \mathbf{q}_w^e \left(\frac{h}{h_r} \right)^{\alpha_{wind}} + \delta \mathbf{q}_w \tag{3.18}$$

$$= \underbrace{\mathbf{q}_w^e \left(\frac{h}{h_r} \right)^{\alpha_{wind}}}_{\text{Wind shear}} + \underbrace{\mathbf{f}_{w,t}(h, \upsilon_{kite}, \theta, \phi, \beta_b)}_{\text{Wind turbulence}} \tag{3.19}$$

Where $\mathbf{q}_w^e$ is the wind vector measured at height h_0 and $\mathbf{f}_{w,t}$ is the wind turbulence function described in Appendix A.

It is reasonable to assume that kite will operate in a environment where the wind vector is dominated by wind in one direction, and the contribution from the other elements of the vector is primarily due to turbulence. Defining the wind along the e^x axis as the primary contributer to the wind vector gives the following approximation:

$$\nu = \sqrt{(\upsilon)_x^2 + \cancel{(\upsilon)_y^2} + \cancel{(\upsilon)_z^2}} = \upsilon_x \tag{3.20}$$

$$\gamma = \arccos \left(\frac{(\delta \upsilon)_z}{\upsilon_x} \right) \tag{3.21}$$

$$\mu = w_\mu = \arctan \left(\frac{(\delta \upsilon)_y}{(\delta \upsilon)_x} \right) \tag{3.22}$$

Redefining γ as the angle between the $x^e y^e$ plane at height h_0 and the wind vector, results in:

$$\gamma = \frac{\pi}{2} - \arccos \left(\frac{(\delta \upsilon)_z}{\upsilon_x} \right) \tag{3.23}$$

$$\mathbf{q}_w^l = \underbrace{(\mathbf{q}_w^e)_x \left(\frac{h}{h_r}\right)^{\alpha_{wind}}}_{\text{Wind shear}} + \underbrace{\mathbf{f}_{w,t}(h, v_{kite}, \theta, \phi, \beta_b)}_{\text{Wind turbulence}} \tag{3.24}$$

$$x_8 = \mathbf{q}_w^l \tag{3.25}$$

The state space representation of the kite model with the new states then is given by:

$$\begin{bmatrix} \dot{x_1} \\ \dot{x_2} \\ \dot{x_3} \\ \dot{x_4} \\ \dot{x_5} \\ \dot{x_6} \\ \dot{x_7} \\ \dot{x_8} \end{bmatrix} = \begin{bmatrix} x_4 \\ x_5 \\ x_6 \\ \left(S^{-1}\frac{F^l}{m} - a\right)_1 \\ \left(S^{-1}\frac{F^l}{m} - a\right)_2 \\ \frac{M_k}{I_k} \\ 0 \\ \dot{x_8} \end{bmatrix} + \begin{bmatrix} 0 \\ 0 \\ 0 \\ 0 \\ 0 \\ 0 \\ b_u \\ 0 \end{bmatrix} u + \begin{bmatrix} w_{x_4} \\ w_{x_5} \\ w_{x_6} \\ w_{\dot{x_4}} \\ w_{\dot{x_5}} \\ w_{\dot{x_6}} \\ w_{\dot{x_7}} \\ w_{\dot{x_8}} \end{bmatrix} \tag{3.26}$$

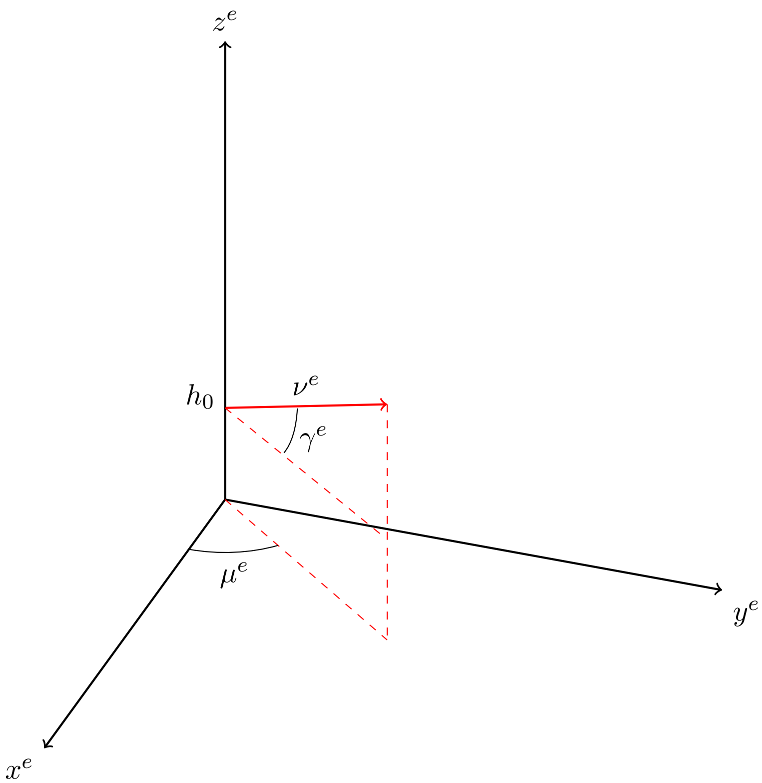

Figure 3.2: Wind direction is represented by μ^e and γ^e while the strength of the wind is represented by ν^e. All coordinates are in earth frame.

4

Observability analysis

The observability problem consists of investigating whether there exist relations binding the state-variables to inputs, outputs and their time derivative thus locally defining them uniquely in terms of measurable quantities without the need for knowing the initial conditions of the states. If no such relation exist, the initial state of the system cannot be deduced strictly by looking at the input-output behavior of the system. [3]

In this chapter the theory behind the observability analysis is first presented in Chapter 4.1 the applied to determine the observability properties of the kite model in Chapter 4.2.

4.1 Nonlinear observability

There are several strategies to determine the observability of a nonlinear system. In this paper the focus will be on the the differential geometric approach as presented in [9, 18, 3].

A nonlinear system is defined as

$$\Sigma : \begin{array}{rl} \dot{\mathbf{x}} = & \mathbf{f}(\mathbf{x}) + \mathbf{g}(\mathbf{x})\mathbf{u} \\ \mathbf{y} = & \mathbf{h}(x) \end{array} \tag{4.1}$$

It is assumed that $\mathbf{x} \in M$ where M is a open subset of $\mathbb{R}^m$. And where $\mathbf{f} \in \mathbb{R}^m$ is the model function, $\mathbf{h} \in \mathbb{R}^n$ is the measurements and $\mathbf{g}(\mathbf{x})\mathbf{u} \in \mathbb{R}^p$ is the contribution of the inputs.

Suppose the trajectories of Σ are required to satisfy the initial condition

$$\mathbf{x}(t_0) = x_0$$

then Σ defines a map from inputs to outputs as follows. Each input $(u(t), [t^0, t^1])$ gives rise to a solution $(\mathbf{x}(t), [t^0, t^1])$ of $\dot{\mathbf{x}} = \mathbf{f}(\mathbf{x}, u(t))$ satisfying the initial condition. The output $(\mathbf{y}(t), [t^0, t^1]$ is then given by $\mathbf{y} = \mathbf{h}(\mathbf{x}(t))$. This map is denoted by

$$\Sigma_{\mathbf{x}^0} : (u(t), [t^0, t^1]) \mapsto (\mathbf{y}(t), [t^0, t^1])) \tag{4.2}$$

and is referred to as the input-output map of Σ at $\mathbf{x}^0$.

A pair of points $\mathbf{x}^0$ and $\mathbf{x}^1$ are indistinguishable (denoted $\mathbf{x}^0\mathbf{I}\mathbf{x}^1$) if $(\Sigma, \mathbf{x}^0)$ and $(\Sigma, \mathbf{x}^1)$ realize the same input-output map, that is if: [9]

$$\Sigma_{\mathbf{x}^0} : (u(t), [t^0, t^1]) = \Sigma_{\mathbf{x}^1} : (u(t), [t^0, t^1]) \tag{4.3}$$

Σ is said to be observable at x^0 if $\mathbf{I}(\mathbf{x}^0) = \{\mathbf{x}^0\}$ and observable if $\mathbf{I}(\mathbf{x}) = \{\mathbf{x}\}$ for every $\mathbf{x} \in M$.

In practice however it may not be necessary to distinguish $\mathbf{x}^0$ for every point in M. Distinguishing it from its neighbors may suffice. If there exists a an open neighborhood U of $\mathbf{x}^0$ such that $\mathbf{I}(\mathbf{x}^0) \cap U = \{\mathbf{x}^0\}$, Σ is said to be weakly observable (or distinguishable) at $\mathbf{x}^0$ and locally weakly observable if this the case for every $x \in M$ [9].

4.2 Observability of the kite model

In this chapter the observability properties of the kite system with ground based measurements is investigated. As mentioned in Chapter 1.1, the measurements available from the ground is:

$$\mathbf{h} = \begin{bmatrix}\theta & \phi & \dot{\theta} & \dot{\phi} & \delta_l & \mathbf{q}_w^e\end{bmatrix}^T \tag{4.4}$$

The only input in the system is the angular velocity of the flaps controlled by the power cables:

$$\mathbf{g} = \dot{\delta}_l \tag{4.5}$$

Hence for the system to be observable, β_b and $\dot{\beta}_b$ needs to be uniquely identified given only the mentioned inputs and outputs. Recalling from Chapter 2.1:

$$\begin{aligned} M_k &= \frac{1}{2}\rho_{air}(q_w^l)^2 bA(-c_{ks}\beta_s + c_{k,\delta c}\delta_l) - c_{kd}\dot{\beta}_b \\ \dot{\beta}_b &= \frac{1}{c_{kd}}\left(\frac{1}{2}\rho_{air}(q_w^l)^2 bA(-c_{ks}\beta_s + c_{k,\delta c}\delta_l)\right) - M_k \end{aligned} \tag{4.6}$$

As δ_l is a measured state and the rest of the parameters is assumed known, it is only necessary to determine the effect of the side slip β_s and the relative wind $\mathbf{q}_w^l$ to obtain the value of $\dot{\beta}_b$, recalling from Chapter 2.1:

$$\beta_s = -\arcsin\left(\frac{c(\beta_b)((\mathbf{q}_w^l)_x s(\phi) + rs(\theta)\dot{\phi}) + s(\beta_b)((\mathbf{q}_w^l)_x c(\theta)c(\phi) - r\dot{\theta})}{\sqrt{((\mathbf{q}_w^l)_x c(\theta)c(\phi))^2 + ((\mathbf{q}_w^l)_x s(\phi) + rs(\theta)\dot{\phi})^2}}\right) \tag{4.7}$$

where $(\mathbf{q}_w^l)_x$ is the wind contribution in the e^x direction given in the local frame given by:

$$\mathbf{q}_w^l = R_e^l \left((\mathbf{q}_w^e)_y \left(\frac{h}{h_r}\right)^{\alpha_{wind}} + \mathbf{f}_{w,t}(h, v_{kite}, \theta, \phi, \beta_b) \right) - \dot{p}^l \tag{4.8}$$

The turbulence contribution $\mathbf{f}_{w,t}$ is also dependent on the yaw of the kite. It is clear that β_b is needed to calculate $\dot{\beta}_b$. Recalling again from Chapter 2.1,the relation between the earth frame and the wind frame is given by:

$$R_e^w = R_e^l R_l^b R_b^w \tag{4.9}$$

$$= \underbrace{R_x(\theta)R_z(\phi)R_z}_{\text{Known}} \underbrace{(\beta_b)R_y}_{\text{Unknown}} \underbrace{(\alpha_w)R_z(\beta_w)}_{\text{Known}} \tag{4.10}$$

It is possible to calculate β_s by using the relation of the wind frame, local frame and the body frame given by:

$$R_w^b = (R_b^w)^T = R_l^b R_w^l \tag{4.11}$$

$$= \begin{pmatrix} \cos(\alpha_w)\cos(\beta_s) & -\sin(\beta_s) & \sin(\alpha_w)\cos(\beta_s) \\ \cos(\alpha_w)\sin(\beta_s) & \cos(\beta_s) & \sin(\alpha_w)\sin(\beta_s) \\ -\sin(\alpha_w) & 0 & \cos(\alpha_w) \end{pmatrix} \tag{4.12}$$

Having calculated β_s, and q_w^l it is possible to calculate β_b. However since α_w and β_s are given by the the relative wind which in turn is given by the yaw of the kite, it is not possible to calculate $\beta_{b,0}$ directly. But by making the assumption that the wind vector is being dominated by the wind in e^x-direction and the contribution of the turbulence is negligible we are able to give a approximate value $\hat{\beta}_{b,0}$ of $\beta_{b,0}$ since:

$$\begin{aligned}
\mathbf{q}_w^l =& R_e^l \left((\mathbf{q}_w^e)_y \left(\frac{h}{h_r}\right)^{\alpha_{wind}} + \cancel{\mathbf{f}_{w,t}(h, v_{kite}, \theta, \phi, \beta_b)} \right) - \dot{p}^l \\
=& R_e^l (\mathbf{q}_w^e)_y \left(\frac{h}{h_r}\right)^{\alpha_{wind}} - \dot{p}^l
\end{aligned} \tag{4.13}$$

As the relative wind is no longer dependent on the yaw, but purely on the height of the kite it is now possible to find $\hat{\beta}_{b,0}$ by using the relations given in 4.6, 4.7 and 4.12. This value of $\beta_{b,0}$ will however include an error due to the exclusion of the wind turbulence.

5

State estimation

A state observer is a system that estimates the states of a process given only access to the process inputs and outputs. This a trivial matter when the process is linear. When the system is non linear however the task of estimating the states becomes more complex. The optimal solution to the non linear state estimation problem requires the propagation of the full Probability Density Function (PDF). The PDF is defined as the derivative of the cumulative distribution function [14]. Since the form of the PDF is not restricted it cannot, in general,be described using a finite number of parameters. The use of approximations is therefor necessary in the design of any practical state estimator. One of the most widely used state estimator algorithms is the Kalman Filter (KF), it only utilizes the mean and covariance of the state in its update rule which makes it computationally manageable and require few special assumptions about the form of the process.[11]

In 5.1 the idea behind the KF is demonstrated. In 5.2 and 5.3 two different non linear KF's is presented namely the Extended Kalman Filter (EKF) and the Unscented Kalman Filter (UKF).

5.1 Discrete Kalman filter

A discrete model of a linear system is defined as [22]:

$$x_k = F_k x_{k-1} + B_k u_k + w_k \tag{5.1}$$

$$y_k = H_k x_k + v_k \tag{5.2}$$

Where F_k is the state transition model which relates the previous time step state vector (x_{k-1}) to the next time step (x_k), B_k is the control-input model, w_k is the process noise which is assumed to be drawn from a zero mean multivariate distribution with covariance Q_k:

$$w_k \sim N(0, Q_k) \tag{5.3}$$

H_k is the observation model, and v_k is the observation noise which is assumed to be zero mean Gaussian white noise with covariance R_k:

$$v_k \sim N(0, R_k) \tag{5.4}$$

A initial estimate of the state vector is assumed to be known and declared as $\hat{x}_k^-$, this is known as the a priori estimate of the state vector. The error of this a priori estimate is given by:

$$e_k^- = x_k - \hat{x}_k^- \tag{5.5}$$

The covariance matrix of the error is given by:

$$P_k^- = E[e_k^- e_k^{-T}] = E[(x_k - \hat{x}_k^-)(x_k - \hat{x}_k^-)^T] \tag{5.6}$$

The measurement vector (y_k) is then used to update the state estimate

$$\hat{x}_k = \hat{x}_k^- + K_k(y_k - H_k\hat{x}_k^-) \tag{5.7}$$

$$\hat{x}_k = \hat{x}_k^- + K_k(H_k x_k + v_k - H_k\hat{x}_k^-) \tag{5.8}$$

K_k is the Kalman gain and is yet to be found. By substituting (5.8) in to (5.6) the updated (a posteriori) error covariance matrix estimate is found:

$$P_k = E[e_k e_k^T] = E[(x_k - \hat{x}_k)(x_k - \hat{x}_k)^T] \tag{5.9}$$

$$\begin{aligned} P_k = E\{&[(x_k - \hat{x}_k^-) - K_k(H_k x_k + v_k - H_k\hat{x}_k^-)] \\ &[(x_k - \hat{x}_k^-) - K_k(H_k x_k + v_k - H_k\hat{x}_k^-)]^T\} \end{aligned} \tag{5.10}$$

Noting that the a priori state estimate is uncorrelated with the measurement error v_k, the updated error covariance may be written as:

$$P_k = (I - K_k H_k)P_k^-(I - K_k H_k)^T + K_k R_k K_k^T \tag{5.11}$$

Finding the optimal blending factor is done by finding the K_k that minimizes the estimation error variances for the elements of the state vector being estimated. These elements are found along the major diagonal of P_k. By differentiating the trace of P_k w.r.t. K_k and setting the derivative to zero the optimal blending factor, known as the Kalman gain, is given:

$$\frac{d(\text{trace}P_k)}{dK_k} = -2(H_k P_k^-)^T + 2K_k(H_k P_k^- H_k^T + R_k)$$

$$K_k = P_k^- H_k^T (H_k P_k^- H_k^T + R_k)^{-1} \tag{5.12}$$

5.2 Extended Kalman filter

The kite is modeled by a non linear system and the transitions models is therefor not available and needs to be approximated before a Kalman filter may be implemented. A Kalman filter that linearizes about the current mean and covariance is referred to as an extended Kalman filter (EKF).[22] However since the kite-model is somewhat complex the exact Jacobian is not easily available and heavy computation is needed to obtain it. An approximated Jacobian of the state and measurement transformation matrices is therefor computed using Newton's difference quotient.

$$\mathbf{A}_k \approx \frac{\mathbf{f}(\mathbf{x}_k + \Delta, \mathbf{u}) - \mathbf{f}(\mathbf{x}_k, \mathbf{u})}{\Delta} \tag{5.13}$$

$$\mathbf{H}_k \approx \frac{\mathbf{h}(\mathbf{x}_k + \Delta, \mathbf{u}) - \mathbf{h}(\mathbf{x}_k, \mathbf{u})}{\Delta} \tag{5.14}$$

The approximated state vector along with the updated error covariance matrix is computed as shown in Table 5.1.

In the EKF the state distribution is approximated by a Gaussian random variable (GRV), which in turn is propagated analytically through the first order linearization of the non linear system. This is equivalent to applying the linear Kalman filter covariance update equations to the linearized system. The EKF may therefor be seen as providing "first-order" approximations to the optimal covariance matrix and Kalman gain. This might result in large estimate errors and even divergence. [21]

Step		*Equations*
Initialization step		
Design matrices	$\mathbf{Q}(k) =$	$\mathbf{Q}^T > 0$, $\mathbf{R}(k) = \mathbf{R}^T > 0$
Initial conditions	$\hat{\mathbf{x}}_0 =$	$\mathbb{E}[\mathbf{x}_0]$, $\mathbf{P}_0 = \mathbb{E}[(\mathbf{x}_0 - \hat{\mathbf{x}}_0)(\mathbf{x}_0 - \hat{\mathbf{x}}_0)^T]$
Time update		For $k \in \{1, ..., \infty\}$
Model update	$\hat{\mathbf{x}}_k^- =$	$\mathbf{f}[\hat{\mathbf{x}}_{k-1}, \mathbf{u}_{k-1}]$
A priori covariance	$\mathbf{P}_k^- =$	$\mathbf{A}_k \mathbf{P}_{k-1} \mathbf{A}_k^T + \mathbf{Q}$
Measurement update:		
Kalman gain	$\mathbf{K}_k =$	$\mathbf{P}_k^- \mathbf{H}_k^T (\mathbf{H}_k \mathbf{P}_k^- \mathbf{H}_k^T + \mathbf{R})^{-1}$
A posteriori estimate	$\hat{\mathbf{x}}_k =$	$\hat{\mathbf{x}}_k^- + \mathbf{K}_k (\mathbf{y}_k - \mathbf{h}[\hat{\mathbf{x}}_k^-])$
Updated error covariance	$\mathbf{P}_k =$	$(\mathbf{I} - \mathbf{K}_k \mathbf{H}_k) \mathbf{P}_k^-$

Table 5.1: Standard EKF algorithm

5.3 Unscented Kalman filter

To address the weaknesses of the EKF, a new strategy for computing the posterior first and second order statistics (mean, standard deviation and variation) of a random variable introduced into a non linear system is needed. A way of avoiding the linearization of the non linear system is to realize that it is easier to approximate a probability distribution than it is to approximate an arbitrary non linear function or transformation [19].

A way of approximating the probability distribution is to use the Sigma-point approach. In the Sigma-point approach the state distribution is represented by GRV specified using a minimal set of deterministically chosen weighted sample points called sigma-points. These points captures the true mean and covariance of the prior random variable, and when propagated through the true non linear system, captures the posterior mean and covariance to 2nd order (Taylor series expansion) for any non linearity. [11]

The sigma point approach is summarized in three steps:

1. The sigma points are calculated using the mean and square root decomposition of the covariance matrix of the prior random variable.

2. The sigma points are the propagated through the true non linear function.

3. The posterior statistics are calculated using weighted sample mean and covariance of the posterior sigma points

The Unscented Kalman Filter (UKF) uses the sigma point approach as shown in Table 5.2. Where the weights are given by:

$$W_0^{(m)} = \frac{\lambda}{(L+\lambda)} \tag{5.15}$$

$$W_0^{(c)} = \frac{\lambda}{(L+\lambda)} + (1 - \alpha_{UKF}^2 + \beta_{UKF}) \tag{5.16}$$

$$W_i^{(m)} = W_i^c = \frac{1}{2(L+\lambda)} \quad i = 1, \cdots, 2L \tag{5.17}$$

Here L is the number of states. $\lambda = L(\alpha_{UKF}^2 - 1)$, α_{UKF} and β_{UKF} are scaling parameters. α_{UKF} is used to determine the spread of the sigma points around the mean and is typically set to $10^{-4} \leq \alpha_{UKF} \leq 1$. β_{UKF} is used to incorporate prior knowledge of the distribution of the states (for Gaussian distribution, $\beta_{UKF} = 2$ is optimal). [20]

It has been shown that the EKF and the UKF have a similar computational complexity of $\mathcal{O}(L^3)$. [20]

Step		*Equations*
Initialization step		
Design matrices	$\mathbf{Q}(k) =$	$\mathbf{Q}^T > 0$, $\mathbf{R}(k) = \mathbf{R}^T > 0$
Initial conditions	$\hat{\mathbf{x}}_0 =$	$\mathbb{E}[\mathbf{x}_0]$, $\mathbf{P}_0 = \mathbb{E}[(\mathbf{x}_0 - \hat{\mathbf{x}}_0)(\mathbf{x}_0 - \hat{\mathbf{x}}_0)^T]$
Calculate sigma points		For $k \in \{1, ..., \infty\}$
	$\chi_{k-1} =$	$[\hat{\mathbf{x}}_{k-1} \quad \hat{\mathbf{x}}_{k-1} + \eta\sqrt{\mathbf{P}_{k-1}} \quad \hat{\mathbf{x}}_{k-1} - \eta\sqrt{\mathbf{P}_{k-1}}]$
Time update		
Model update	$\chi_{k\|k-1} =$	$\mathbf{f}[\chi_{k-1}, \mathbf{u}_{k-1}]$
Priori state	$\hat{\mathbf{x}}_k^- =$	$\sum_{i=0}^{2L} W_i^{(m)} \chi_{i,k\|k-1}$
Priori covar.	$\mathbf{P}_k^- =$	$\sum_{i=0}^{2L} W_i^{(c)} [\chi_{i,k\|k-1} - \hat{\mathbf{x}}_k^-][\chi_{i,k\|k-1} - \hat{\mathbf{x}}_k^-]^T + \mathbf{Q}$
Sigma measurement	$\mathcal{Y}_{k\|k-1} =$	$\mathbf{h}[\chi_{i,k\|k-1}]$
Priori measurement	$\hat{\mathbf{y}}_k^- =$	$\sum_{i=0}^{2L} W_i^{(m)} \mathcal{Y}_{k\|k-1}$
Measurement update:		
Posteriori covar.	$\mathbf{P}_{\hat{\mathbf{y}}_\mathbf{k}\hat{\mathbf{y}}_\mathbf{k}} =$	$\sum_{i=0}^{2L} W_i^{(c)} [\mathcal{Y}_{k\|k-1} - \hat{\mathbf{y}}_k^-][\mathcal{Y}_{k\|k-1} - \hat{\mathbf{y}}_k^-]^T + \mathbf{R}$
Posteriori covar.	$\mathbf{P}_{\mathbf{x}_\mathbf{k}\mathbf{y}_\mathbf{k}} =$	$\sum_{i=0}^{2L} W_i^{(c)} [\chi_{i,k\|k-1} - \hat{\mathbf{x}}_k^-][\mathcal{Y}_{k\|k-1} - \hat{\mathbf{y}}_k^-]^T$
Kalman gain	$\mathcal{K} =$	$\mathbf{P}_{\mathbf{x}_\mathbf{k}\mathbf{y}_\mathbf{k}} \mathbf{P}_{\hat{\mathbf{y}}_\mathbf{k}\hat{\mathbf{y}}_\mathbf{k}}^{-1}$
Posteriori estimate	$\hat{\mathbf{x}}_k =$	$\hat{\mathbf{x}}_k^- + \mathcal{K}(\mathbf{y}_k - \hat{\mathbf{y}}_k^-)$
Updated error covar.	$\mathbf{P}_k =$	$\mathbf{P}_k^- - \mathcal{K}_k \mathbf{P}_{\hat{\mathbf{y}}_\mathbf{k}\hat{\mathbf{y}}_\mathbf{k}} \mathcal{K}_k^T$

Table 5.2: Standard UKF algorithm

6

Simulation

The simulations was conducted in MATLAB and Simulink. The parameters used in all simulations is given in Appendix C unless other is noted. Three cases where the yaw angle of the process is set to follow different paths are chosen as they represent widely different dynamics of the process:

Case 1: The yaw angle of the kite is set to: $\beta_b = 0$. The kite will in this case drift to a equilibrium.

Case 2: The yaw angle of the kite is set to: $\beta_b = \frac{40\pi}{180}\sin(0.75t)$ The kite will in this case drift along the y^e axis as β_b never exceed $\frac{\pi}{2}$.

Case 2: The yaw angle of the kite is set to: $\beta_b = \frac{100\pi}{180}\sin(1.5t)$ The kite will in this case follow a trajectory resembling the infinity symbol. This is a well known kite power trajectory and results in high kite speeds.

The yaw angle β_b and the trajectory of the kite in the three cases is depicted in Figure 6.1.

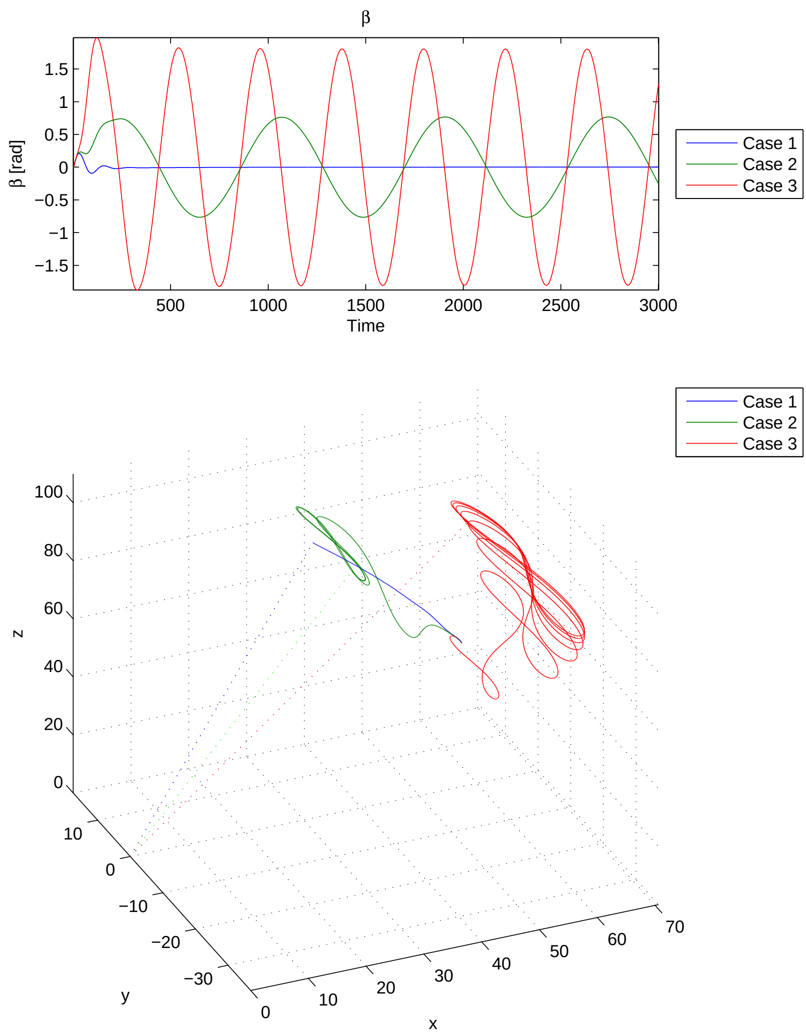

Figure 6.1: Process trajectory - β_b and trajectory of the process for three cases

6.1 UKF vs EKF

The purpose of this series of simulations is to test and compare the EKF and UKF's ability to approximate β_b and $\dot{\beta}_b$ during different dynamics of operation. q_w^e is set constant to $[6, 0, 0]^T$ and the effect of turbulence is neglected.

Figure 6.2 shows the EKF and UKF approximated as well as the real process yaw angle during the three cases mentioned above.

Figure 6.3 shows the approximated as well as the real process yaw angular velocity.

The mean squared error (MSE) of the EKF and UKF approximated θ, ϕ and β_b from all of the simulations where the yaw angle sinus varies according to Table C.1, are shown in Table 6.1.

Variable	**MSE (mean) EKF**	**MSE (var) EKF**
θ	0.0051	$4.1562 \cdot 10^{-4}$
ϕ	0.0064	$3.2196 \cdot 10^{-4}$
β_b	0.7138	6.0507
	MSE (mean) UKF	**MSE (var) UKF**
θ	$1.0888 \cdot 10^{-6}$	$2.0583 \cdot 10^{-12}$
ϕ	$2.7603 \cdot 10^{-6}$	$1.3493 \cdot 10^{-11}$
β_b	0.0106	$1.8724 \cdot 10^{-4}$

Table 6.1: MSE of EKF and UKF of system without wind turbulence

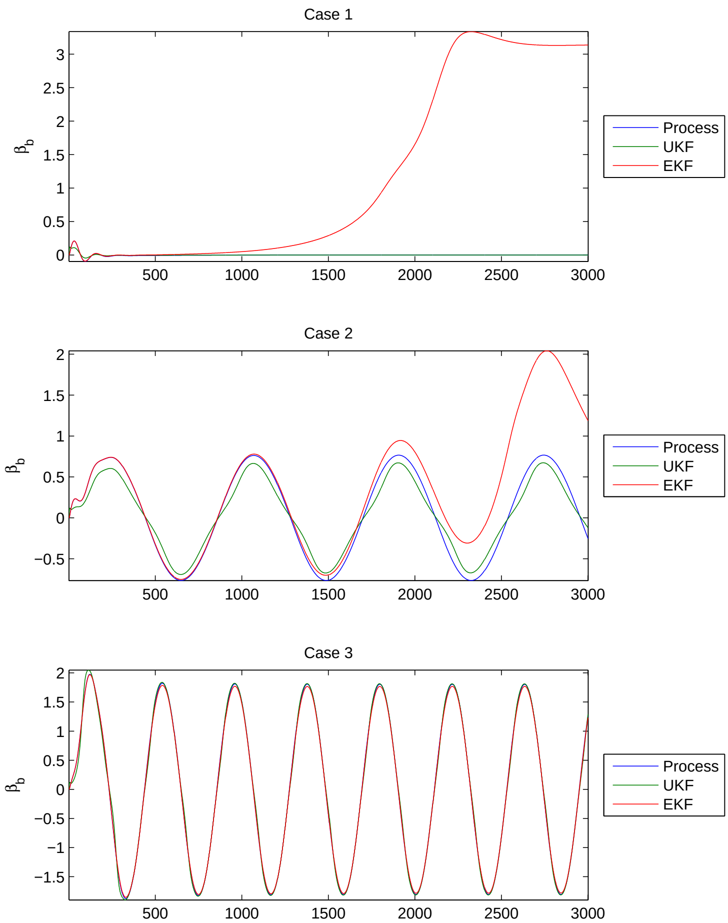

Figure 6.2: UKF and EKF approximated β_b - The UKF and EKF approximated β_b in the different cases

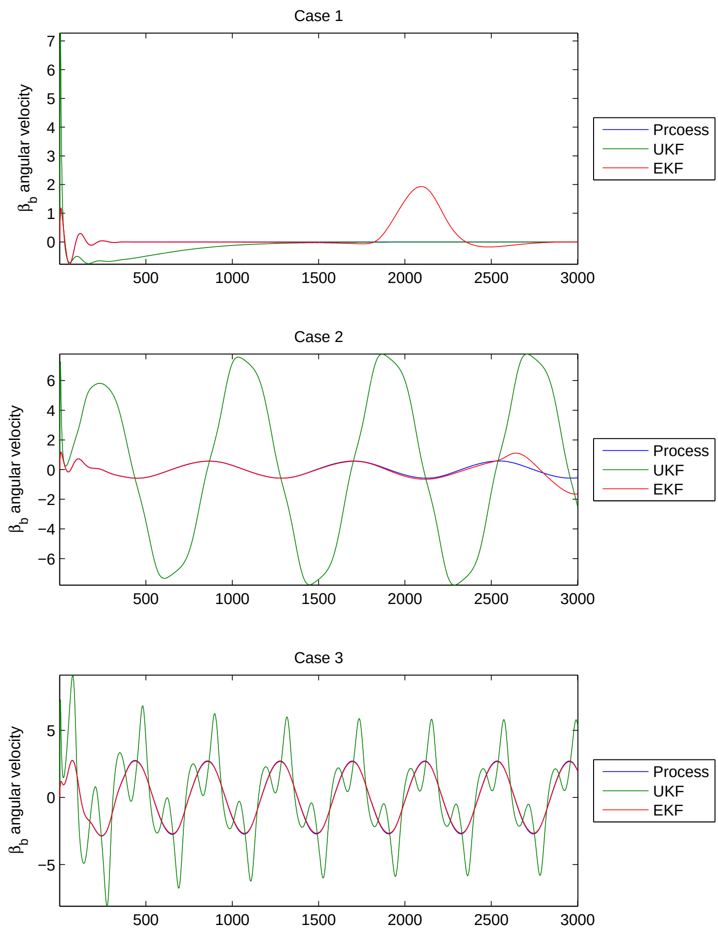

Figure 6.3: UKF and EKF approximated $\dot{\beta}_b$ - The UKF and EKF approximated $\dot{\beta}_b$ in the different simulations

Where the MSE is defined as:

$$MSE = \sum_{i=1}^{N} (x - \hat{x})^2 \tag{6.1}$$

where N is the number of sample points and. The MSE shown in Table 6.1 is then calculated by taking the mean of every time series MSE.

As seen by Table 6.1 and Figure 6.2 the UKF outperforms the EKF quite clearly when it comes to estimating the yaw of the kite (β_b). The EKF fails when the process is experiencing low or dynamic operation. This was expected due to the EKF use of the approximated Jacobian to calculate the error covariance and Kalman gain. Because it uses a approximated Jacobian of the process it does however perform better at estimating the angular velocity of the yaw than the UKF. Because the EKF is "bounded" by the approximated Jacobian it does a poor job of estimating dynamics not described by the first derivative of the system which does not influence the Jacobian much but may have a large influence on the overall system over time.

6.2 Wind turbulence response

The purpose of this series of simulation is to test the UKF's ability to estimate β_b under different dynamic of operation with different wind strengths. The wind speed at $h_0 = 2m$ is varied between $5\frac{m}{s}$ (gentle breeze),$10\frac{m}{s}$ (fresh breeze) and $15\frac{m}{s}$ (near gale).[2]

Figure 6.4 shows the estimated yaw angle during different wind speeds for case 1.

Figure 6.5 shows the estimated yaw angle during different wind speeds for case 2.

Figure 6.6 shows the estimated yaw angle during different wind speeds for case 3.

The MSE of the UKF estimated θ, ϕ and β_b are shown in Table 6.2, while plots of the simulated and estimated wind is shown in Appendix B.

As witnessed by Table 6.2 and Figure 6.4- 6.6, the UKF is still able to estimate the yaw with relative small errors.

It is however noticeable that the MSE mean is larger in Case 2 compared to the other cases. This is due to the estimated kite body yaw angular velocity $\dot{\beta}_b$, as previously mentioned, is dependent on three factors, the relative wind q_w^l, the side slip β_s and the flaps angle δ_l. As δ_l is the only known of these factors it follows that the estimated $\dot{\beta}_b$ error grows as the known state contribution decreases in comparison to the estimated ones.

The estimated and simulated wind is shown in Appendix B.2, as expected it is shown that the UKF does a poor job of estimating the wind turbulence. This is due to the turbulence models dependency of β_b and

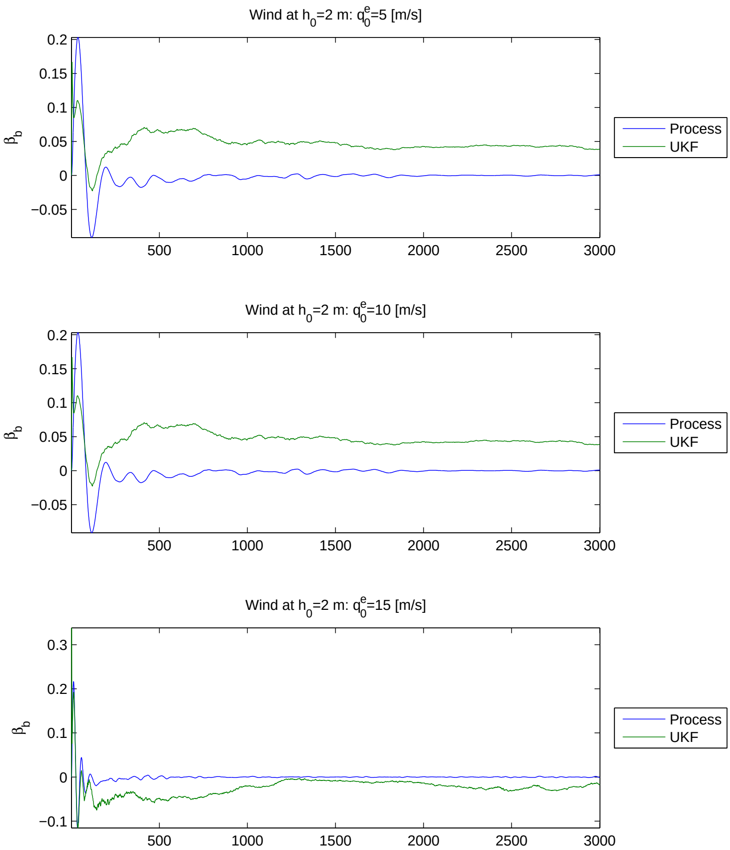

Figure 6.4: UKF estimated β_b for case 1 and turbulence - UKF estimated β_b with constant process yaw angle and various wind speeds

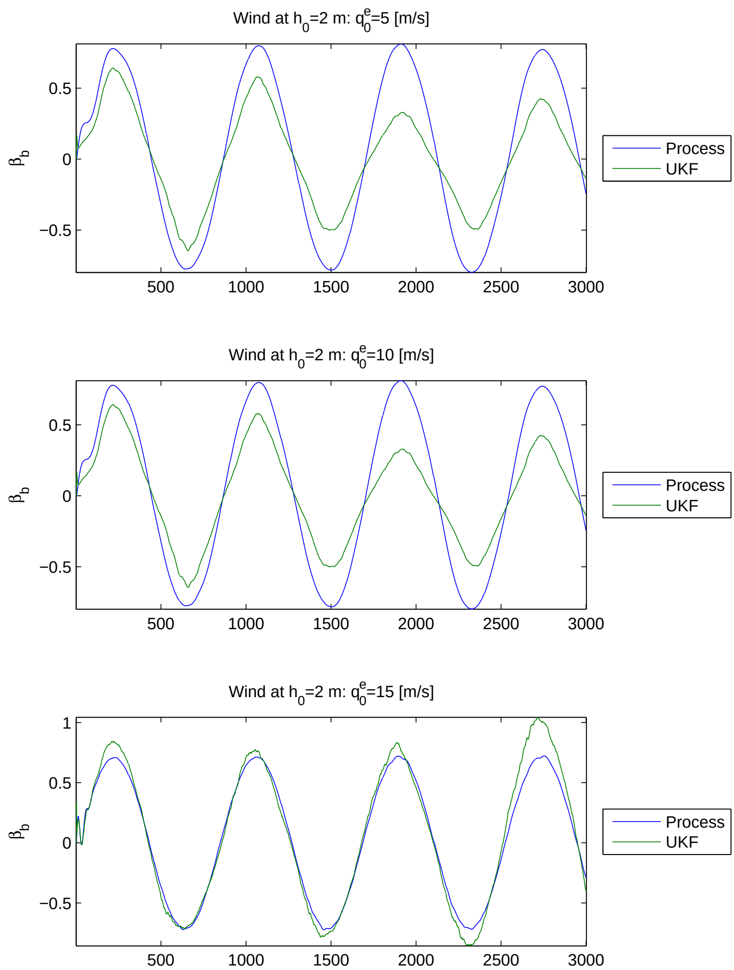

Figure 6.5: UKF estimated β_b for case 2 and turbulence - UKF estimated β_b with process yaw angle given by Case 2 and various wind speeds

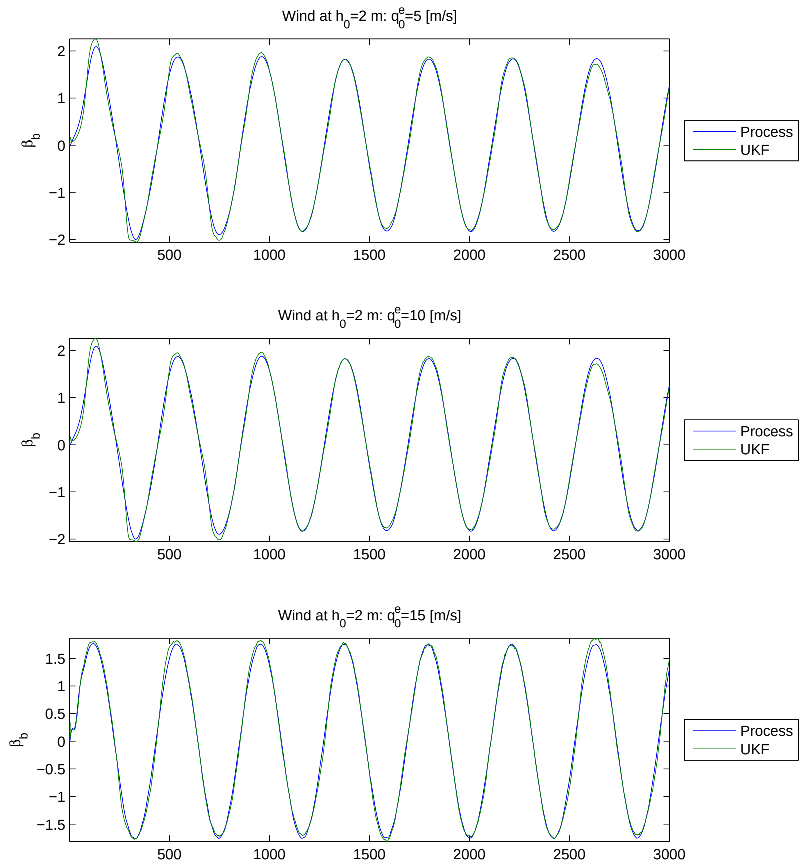

Figure 6.6: UKF estimated β_b for case 3 and turbulence - UKF estimated β_b with process yaw angle given by Case 3 and various wind speeds

	Case 1	
Variable	**MSE (mean)**	**MSE (var)**
θ	$9.6799 \cdot 10^{-8}$	$5.1550 \cdot 10^{-14}$
ϕ	$8.5377 \cdot 10^{-8}$	$3.2133 \cdot 10^{-13}$
β_b	0.0015	$3.0897 \cdot 10^{-6}$
	Case 2	
Variable	**MSE (mean)**	**MSE (var)**
θ	$4.8240 \cdot 10^{-5}$	$3.3282 \cdot 10^{-9}$
ϕ	$3.9483 \cdot 10^{-6}$	$3.1599 \cdot 10^{-11}$
β_b	0.0125	$2.2441 \cdot 10^{-4}$
	Case 3	
Variable	**MSE (mean)**	**MSE (var)**
θ	$6.7121 \cdot 10^{-6}$	$5.8655 \cdot 10^{-11}$
ϕ	$1.7563 \cdot 10^{-5}$	$1.7904 \cdot 10^{-10}$
β_b	0.0060	$1.1255 \cdot 10^{-4}$

Table 6.2: MSE of UKF estimated states with different dynamic of operation and wind strengths

the kite speed. Errors in these states are propagated through the the turbulence model and in combination with the use of random noise results in deviations of the turbulence contribution.

7

Conclusion

In the modeling part of this thesis (Chapter 2- 3) the wind dynamics on an existing kite model was expanded to include the effect of wind shear and turbulence. Although the wind model has not been compared to actual data the simulation shows realistic dynamics compared to existing data [4].

In the observability analysis part (Chapter 4) the kite model is examined using non linear observability theory and found to be observable with the assumption of that the effect of the turbulence is negligible. This is however not a reasonable assumption in some cases, as it was shown in the simulation part of this thesis (Chapter 6) where the estimation error was larger when the effect of side slip is large compared to the control input.

In the state estimation and simulation in Chapter 5 and 6 the EKF and UKF was compared and the UKF was shown to achieve far better estimations than the EKF. The effect of turbulence on the UKF estimate was shown to increase the error somewhat but the UKF still managed to achieve reasonable good kite yaw estimation results.

7. CONCLUSION

8

Discussion and further work

8.1 Discussion

Although the UKF was found to do a decent job of estimating the kite yaw it is likely that the assumptions made in this thesis is too simplistic and does not reflect the real dynamics of the kite. Especially the assumption that the power cable always is fully stretched and adds nothing to the drag may be shown to be unrealistic and needs to be addressed. By adding the complex dynamic of the cable to the system, the direct measurement of spherical coordinates are lost and position estimation of the kite becomes difficult using only ground based measurement. The use of measuring devices attached to the kite seems to fix these problems and seem like a more desirable solution both in terms of added robustness and decreased estimation errors.

8.2 Further work

8.2.1 Cable modeling

The assumption that the cable may be disregarded when describing the dynamics of the system is a naive one. As the cable grows in length it adds substantial mass while creating drag. The cable will also sag at times creating dynamics not included the model presented in this thesis.

8.2.2 Parameter estimation

The parameters used in this thesis are very roughly approximated and is most likely not correct. To achieve smaller parameter errors a strategy for estimating the parameters should be considered.

8.2.3 State estimation with IMU

Although it has been shown in this thesis to be possible to estimate the yaw of the kite using ground based measurement, the use of measurements in the kite system would add robustness and should be

Appendix A

Simulation of wind

The wind is simulated in Simulink as a vector consisting of the effect of wind shear and wind turbulence on the measured wind. The wind shear is calculated as shown in Chapter 3.1, while the effect of wind turbulence is calculated using the Discrete Dryden Wind Turbulence given in the Aerospace blockset in Simulink.

The Dryden wind turbulence model uses the Dryden spectral representation to add turbulence to the model by using band-limited white noise filtered by digital filters finite difference equations. The parameters used in the block is given Table A.1. [13]

Parameters		Comment
Units:	Metric(MKS)	
Specification:	MIL-HDBK-1797	The most recent
Model type:	Dicrete Dryden(+q -r)	
Wind speed:	$q_{w,0}$	Simulation dependent
Wind direction at 6 m:	0	degrees clockwise from north
Probability of exceedance of high-altitude intensity:	$2 \cdot 10^{-1}$	
Scale length at medium/high altitudes (m):	533.4	Default value
Wingspan (m)	b	Given by model
Band limited noise and discrete filter sample time (sec)	T_s	
Noise seeds:	Simulation dependent	

Table A.1: Dryden wind turbulence parameters

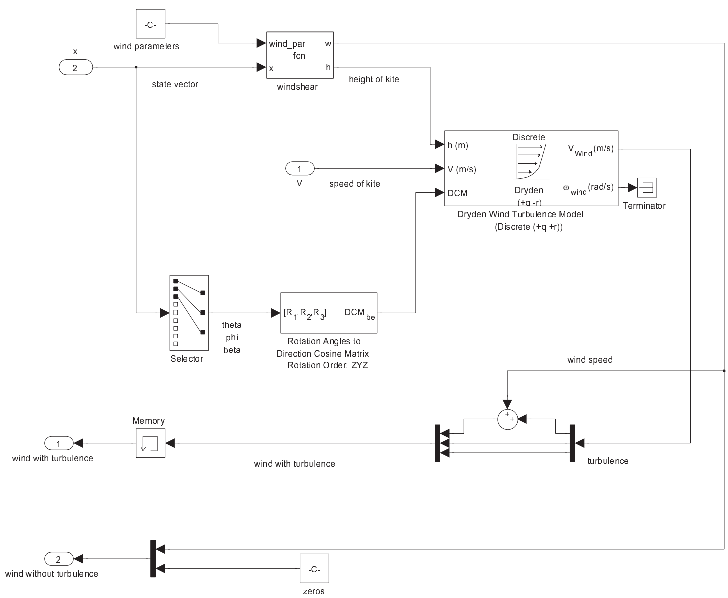

Figure A.1: Simulated wind - Simulink diagram of the wind model, the memory block is to prevent self-reference and adds a time delay of one time step

Appendix B

Plots

B.1 Kite speed

In this section the simulated and UKF estimated kite speed is shown.

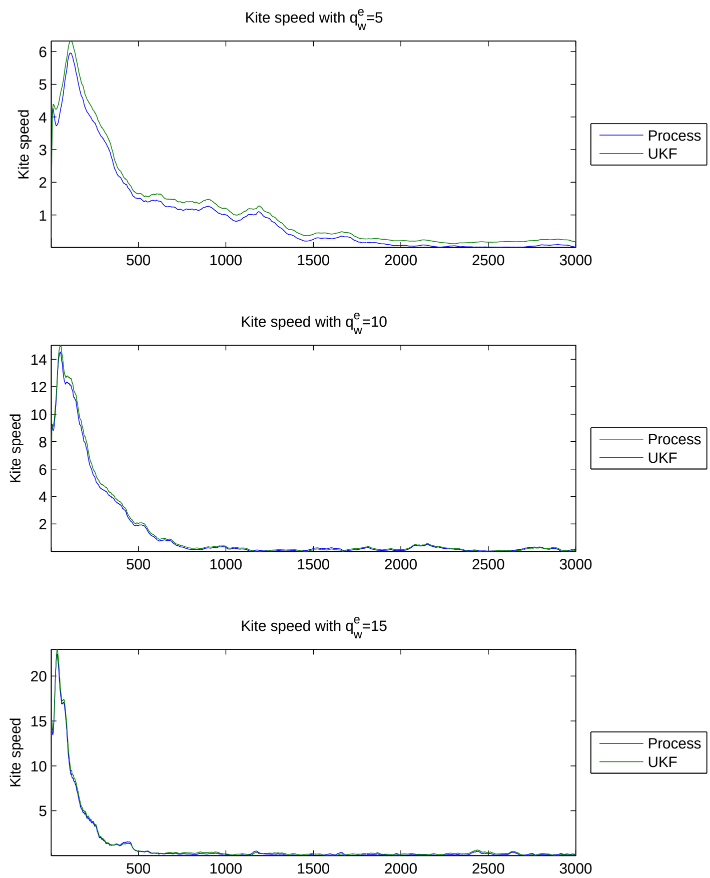

Figure B.1: Kite speed for case 1 - The speed of the kite $[m/s]$ for case 1

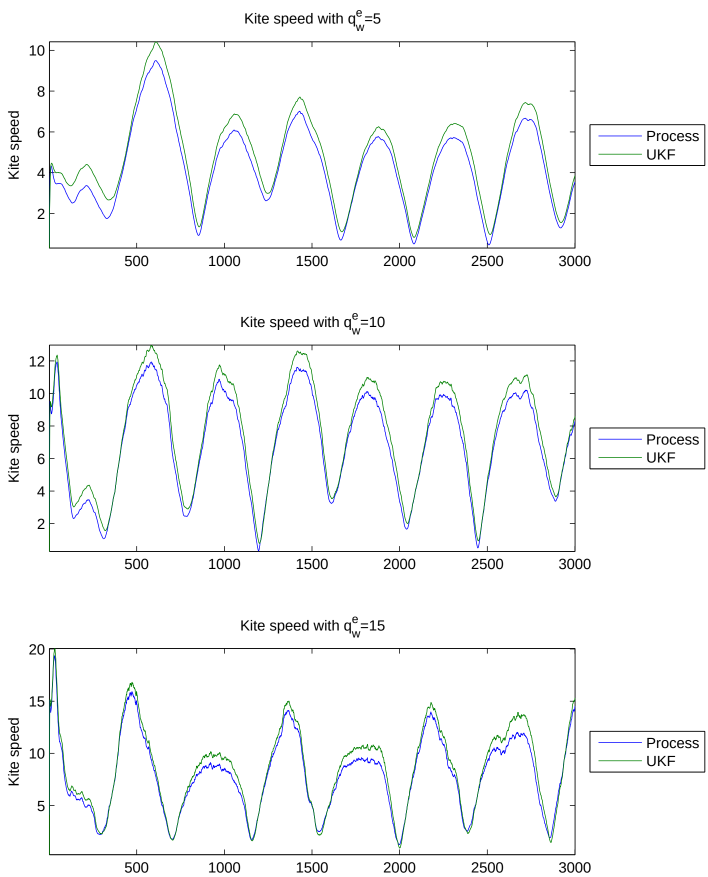

Figure B.2: Kite speed for case 2 - The speed of the kite $[m/s]$ for case 2

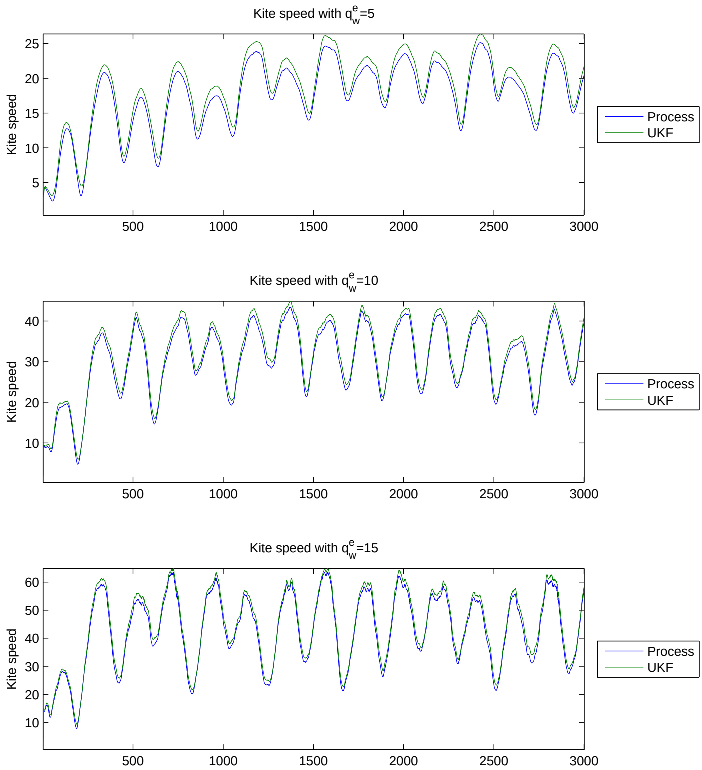

Figure B.3: Kite speed for case 3 - The speed of the kite $[m/s]$ for case 3

B.2 Wind speed

In this section the simulated and UKF estimated wind is shown. As seen by Figure B.4- B.12 the approximated turbulence contribution is not a accurate approximation by any means.

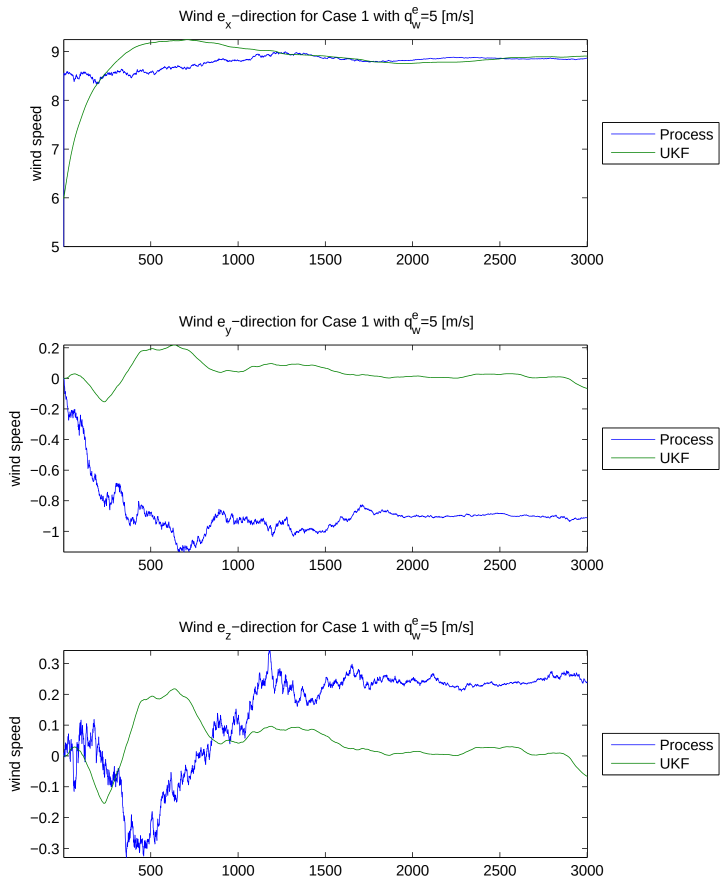

Figure B.4: Wind for case 1, $q_w^e = 5$ - Simulated and UKF estimated wind for case 1

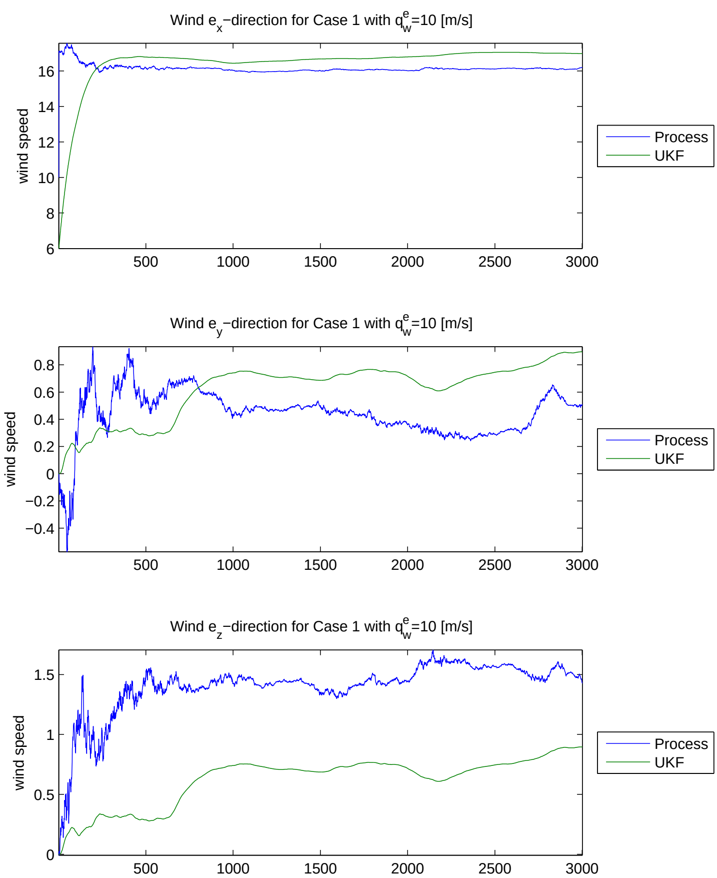

Figure B.5: Wind for case 1, $q_w^e = 10$ - Simulated and UKF estimated wind for case 1

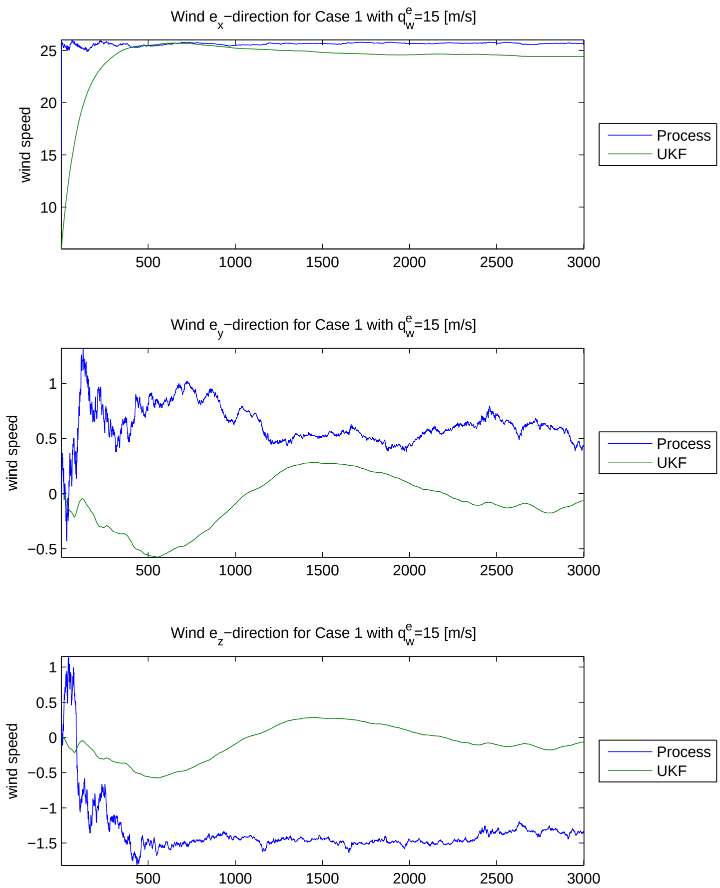

Figure B.6: Wind for case 1, $q^e_w = 15$ - Simulated and UKF estimated wind for case 1

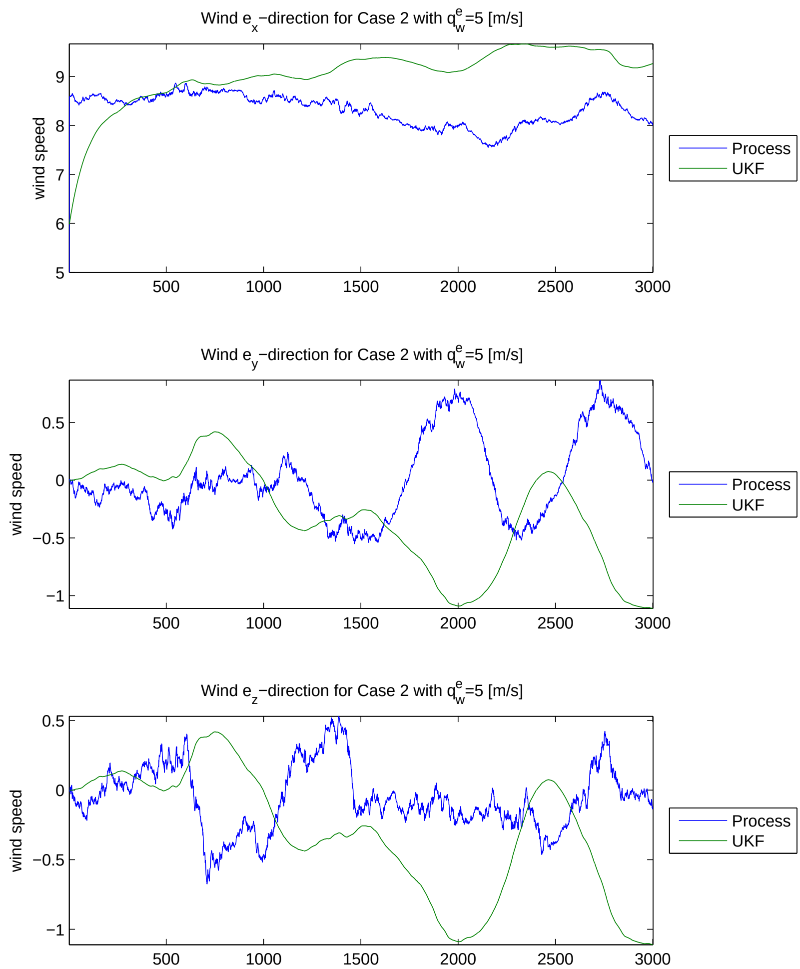

Figure B.7: Wind for case 2, $q_w^e = 5$ - Simulated and UKF estimated wind for case 2

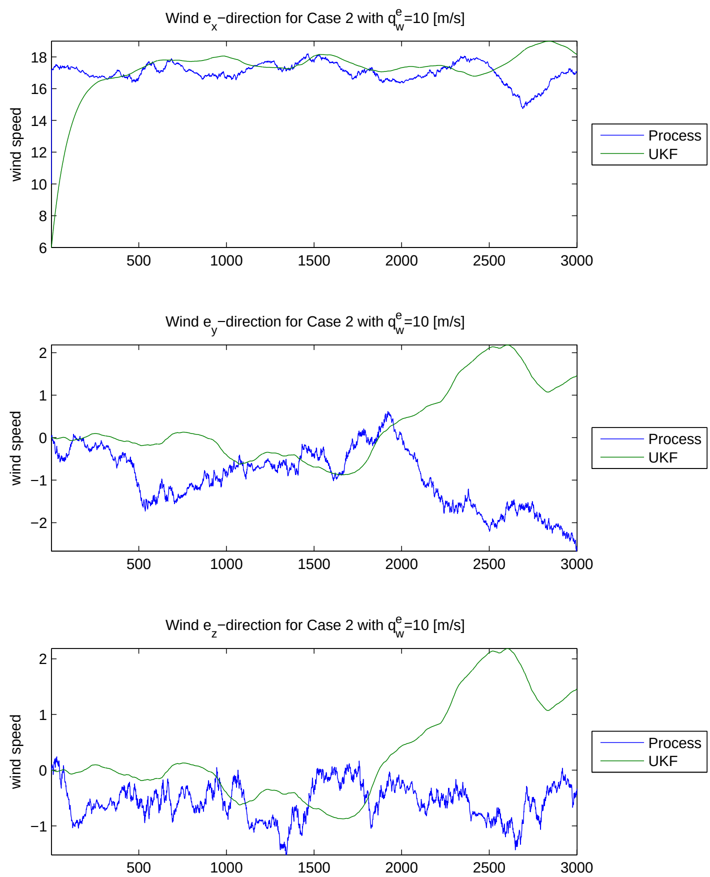

Figure B.8: Wind for case 2, $q_w^e = 10$ - Simulated and UKF estimated wind for case 2

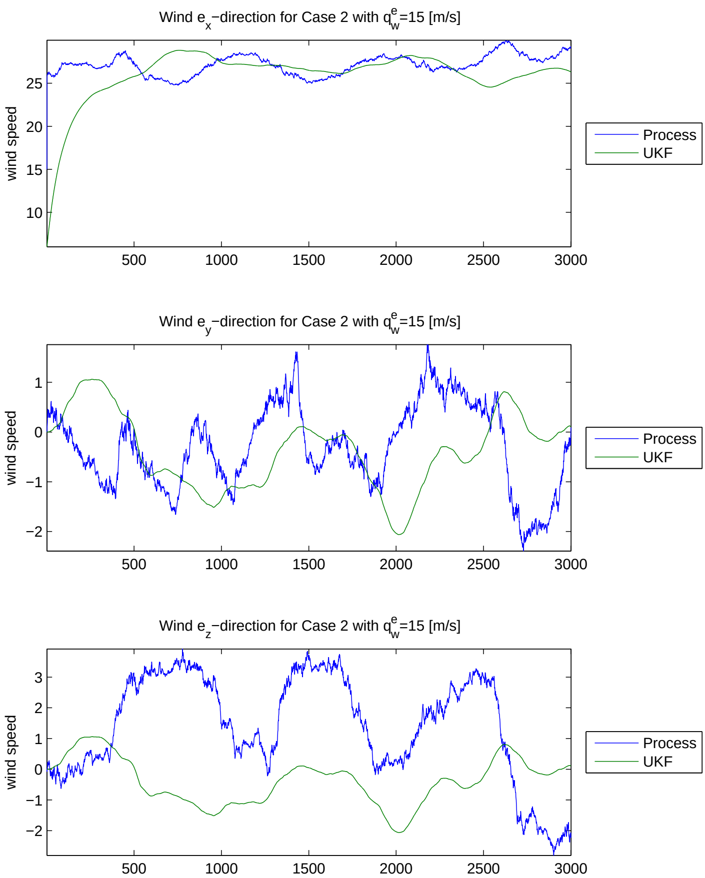

Figure B.9: Wind for case 2, $q_w^e = 15$ - Simulated and UKF estimated wind for case 2

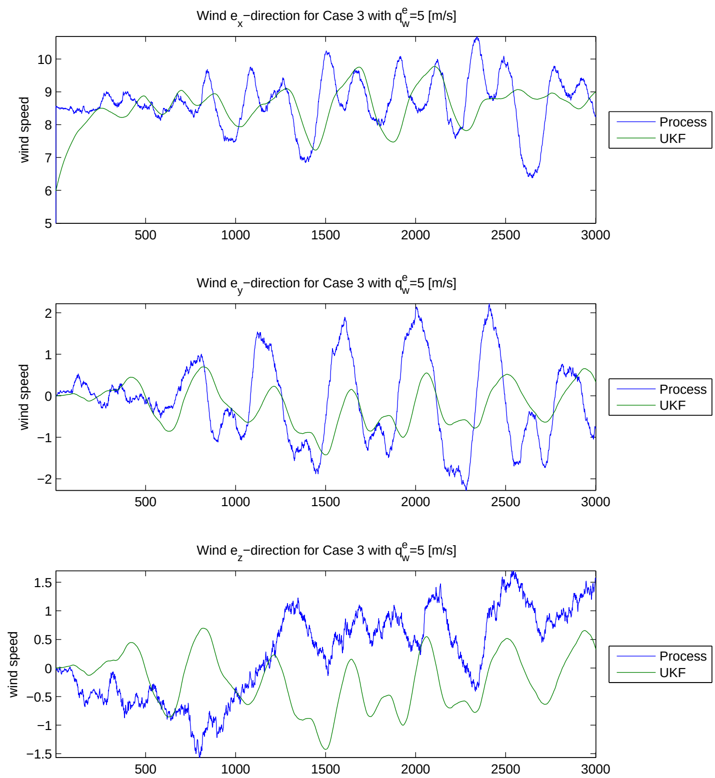

Figure B.10: Wind for case 3, $q_w^e = 5$ - Simulated and UKF estimated wind for case 3

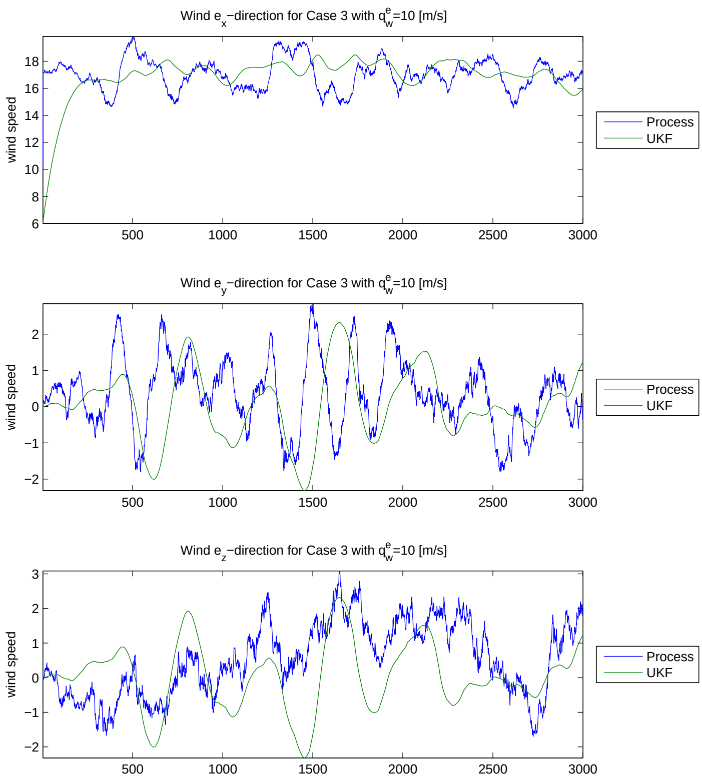

Figure B.11: Wind for case 3, $q_w^e = 10$ - Simulated and UKF estimated wind for case 3

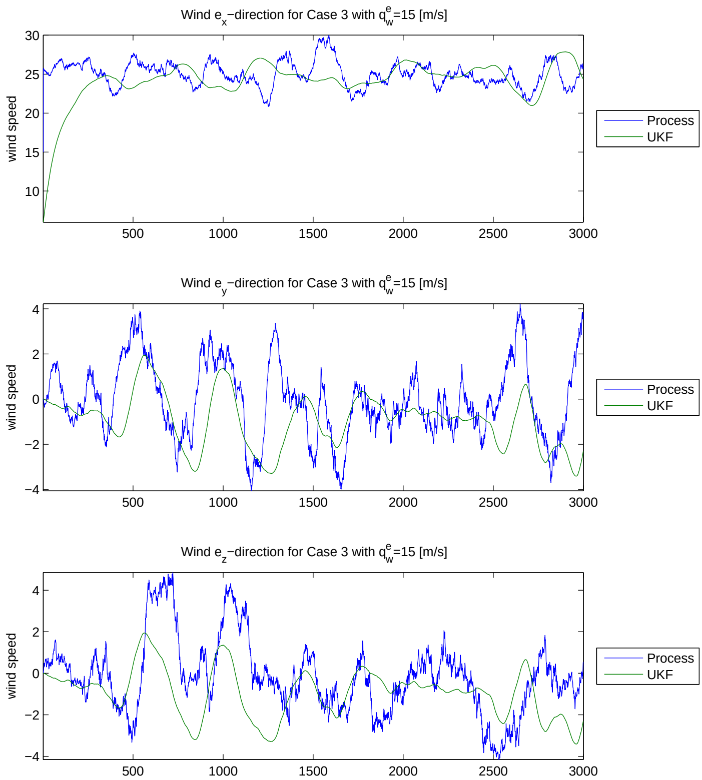

Figure B.12: Wind for case 3, $q_w^e = 15$ - Simulated and UKF estimated wind for case 3

Appendix C

Parameters

C.1 Kalman filter parameters

The state error covariance matrix used both by the EKF and the UKF is given by:

$$\mathbf{Q} = \begin{pmatrix} \frac{\pi}{180} & 0 & 0 & 0 & 0 & 0 & 0 & 0 & 0 & 0 \\ 0 & \frac{\pi}{180} & 0 & 0 & 0 & 0 & 0 & 0 & 0 & 0 \\ 0 & 0 & \frac{2\pi}{180} & 0 & 0 & 0 & 0 & 0 & 0 & 0 \\ 0 & 0 & 0 & \frac{\pi}{180} & 0 & 0 & 0 & 0 & 0 & 0 \\ 0 & 0 & 0 & 0 & \frac{\pi}{180} & 0 & 0 & 0 & 0 & 0 \\ 0 & 0 & 0 & 0 & 0 & \frac{2\pi}{180} & 0 & 0 & 0 & 0 \\ 0 & 0 & 0 & 0 & 0 & 0 & \frac{\pi}{180} & 0 & 0 & 0 \\ 0 & 0 & 0 & 0 & 0 & 0 & 0 & \frac{\pi}{180} & 0 & 0 \\ 0 & 0 & 0 & 0 & 0 & 0 & 0 & 0 & \frac{\pi}{180} & 0 \\ 0 & 0 & 0 & 0 & 0 & 0 & 0 & 0 & 0 & \frac{\pi}{180} \end{pmatrix} \tag{C.1}$$

The measurement error covariance matrix is used both by the EKF and the UKF is given by:

$$\mathbf{R} = \begin{pmatrix} 0.01 & 0 & 0 & 0 & 0 & 0 & 0 & 0 \\ 0 & 0.01 & 0 & 0 & 0 & 0 & 0 & 0 \\ 0 & 0 & 0.01 & 0 & 0 & 0 & 0 & 0 \\ 0 & 0 & 0 & 0.01 & 0 & 0 & 0 & 0 \\ 0 & 0 & 0 & 0 & 0.01 & 0 & 0 & 0 \\ 0 & 0 & 0 & 0 & 0 & 0.01 & 0 & 0 \\ 0 & 0 & 0 & 0 & 0 & 0 & 0.01 & 0 \\ 0 & 0 & 0 & 0 & 0 & 0 & 0 & 0.01 \end{pmatrix} \tag{C.2}$$

The Sigma point tuning parameters used by the UKF is set to:

$$\alpha_{UKF} = 10^{-4} \tag{C.3}$$

$$\beta_{UKF} = 2 \tag{C.4}$$

C.2 Model parameters

The model parameters used in the simulation of the kite is given in Table C.1.

Model parameters		value
Air:		
ρ_{air}	Air density	$1.2\ \frac{kg}{m^3}$
Wind:		
h_0	Wind measurement height	$2\ m$
α_{wind}	Wind shear power law exponent	$\frac{1}{7}$
Kite:		
A	Surface	$10\ m^2$
b	Wingspan	$7\ m$
r	Cable length	$100\ m$
m	Kite mass	10 kg
Drag force:		
C_{dm}:	Minimum drag	0.15
k_d:	Drag constant	0.15
Lift force:		
$C_{L,max}$:	Maximum lift	1.5
c_{ls}:	Lift slope	$1.5\frac{\pi}{C_{L,max}}$
α_0:	De-power angle	$5\frac{\pi}{180}$
Crosswind force:		
c_{cs}:	Crosswind constant	1.1π
Yawing moment:		
c_{ks}:	Directional stability	0.5
$c_{k,\delta,c}$:	Directional stability	0.5
Yaw angle control sinus:		
A_{sin}	Amplitude of sinus	$0 \rightarrow \frac{100\pi}{180}[rad]$
f_{sin}	Frequency of sinus	$0 \rightarrow 2[rad/sec]$

Table C.1: Model parameters

References

[1] Skysails. http://www.skysails.info/index.php?id=472&L=2. 1

[2] Beaufort wind scale. http://www.srh.noaa.gov/mfl/?n=beaufort. 46

[3] M. Anguelova. Nonlinear observability and identifiability, general theory and a case study of a kinetic model. Master's thesis, Chalmers University of technology and Gothenburg University, 2004. 25

[4] D. Bourlis and J. Bleijs. A wind speed estimation method using adaptive kalman filtering for a variable speed stall regulated wind turbine. *PMAPS 2010,IEEE*, 2010. 51

[5] Fagiano L. Canale, M. and M. Milanese. Power kites for wind energy generation. *IEEE Control Systems Magazine*, 2007. 1

[6] H.L Dryden and A.M Kuethe. Effect of turbulence in wind tunnel measurements. *Report no. 342, Bureau of Standards*, 1929. 18

[7] Hugh L. Dryden. Turbulence and diffusion. *Industrial and Engineering Chemistry*, 31(4):416–425, 1939. doi: 10.1021/ie50352a008. 18

[8] L. Fagiano. *Control of Tethered Airfoils for High-Altitude Wind Energy Generation*. PhD thesis, Politecnico Di Torino, 2009. 1

[9] R. Hermann and A. Krener. Nonlinear controllability and observability. *IEE Transactions on Automatic Control, vol Ac-22, No. 5*, 1977. 25, 26

[10] B. Houska. *Robustness and Stability Optimization of Open-Loop Controlled Power Generation Kites*. PhD thesis, Ruprecht-Karls-Universitt Heidelberg, 2007. 1, 18

[11] S.J Julier and J.K. Uhlmann. Unscented filtering and nonlinear estimation. *Proceedings of the IEEE, Vol.92, No. 3*, 2004. 31, 36

[12] H. Knappskog. Nonlinear control of tethered airfoils. Master's thesis, NTNU, 2010. 5, 12

[13] *MATLAB manual, Aerospace Blockset*. Mathworks, 2010a edition, 2010. 55

[14] Emanuel Parzen. On estimation of a probability density function and mode. *The Annals of Mathematical Statistics*, 33(3):pp. 1065–1076, 1962. ISSN 00034851. URL http://www.jstor.org/stable/2237880. 31

[15] A.R Podgaets and W.J. Ockels. Flight control and stability of a multiple kites tethered system. In *Proceedings of Renewable Energy Conference 2006*, pages 1–4, 2006. 1

[16] A.R Podgaets and W.J. Ockels. Flight control of the high altitude wind power system. In *Proceedings of the 7th conference on sustainable application for tropical island states*, pages 1–6, 2007. 1

[17] Rogers A.L. Ray, M.L and J.G. McGowan. Analysis of wind shear models and trends in different terrains. In *American Wind Energy Association Windpower 2006*, 2006. 1, 16

[18] W. Respondek. Introduction to geometric nonlinear control; linerization, observability, decoupling. Lecture given at the Summer School on Mathematical Control Theory, Trieste, 2001. Laboratoire de Mathmatiques, INSA de Rouen, France. 25

[19] J.K Uhlman. *Simultaneous map building and localization for real time applications*. PhD thesis, Univ. Oxford, Oxford, U.K., 1994. 35

[20] R. van der Merwe and E. Wan. The square-root unscented kalman filter for state and parameter estimation. In *Proceedings of the International Conference on Acoustics, Speech, and Signal Processing (ICASSP)*, Salt Lake City, Utah, May 2001. IEEE. URL `http://cslu.cse.ogi.edu/publications/ps/merwe01a.ps.gz`. 36, 37

[21] R. van der Merwe, E.A. Wan, and S.I. Julier. Sigma-point kalman filters for nonlinear estimation and sensor-fusion: Applications to integrated navigation. In *Proceedings of the AIAA Guidance, Navigation & Control Conference*, pages 16–19, 2004. 34

[22] G. Welch and G. Bishop. An introduction to the kalman filter. Course booklet, 2006. 32, 34